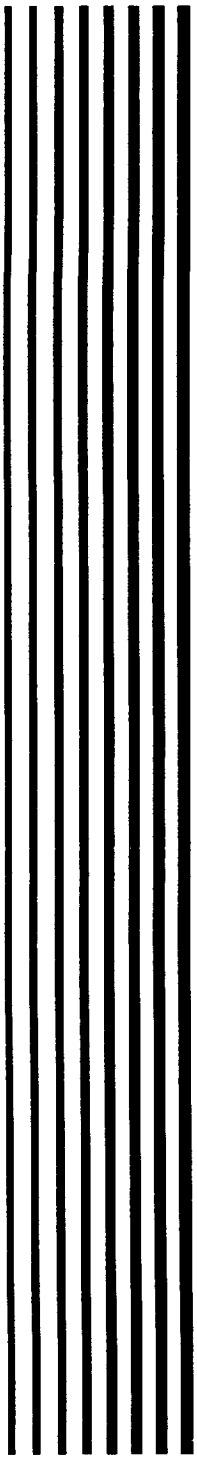

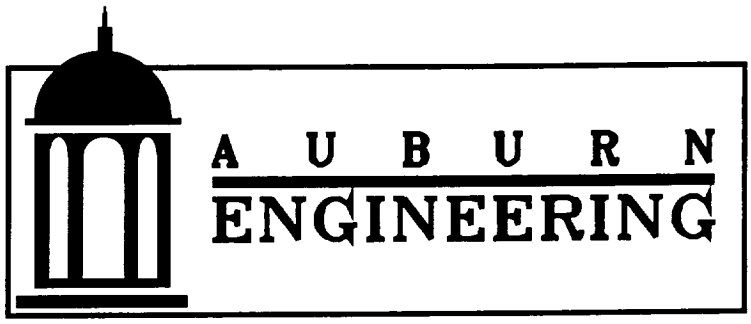

Numerical Investigation of Thermal Stress Convection in Nonisothermal Gases under Microgravity Conditions

Contract NAG3–1882

Final Report

D. W. Mackowski, PI
Mechanical Engineering Department
College of Engineering
Auburn University, AL

Contract Period: 6/1/96–5/31/99

Dr. R. Balasubramaniam, Technical Officer
NCMR, NASA John H. Glenn Research Center

1 Report Summary

1.1 Overview

Reported here are our results of our numerical/theoretical investigation into the effects of thermal stress in nonisothermal gases under microgravity conditions. The first part of the report consists of a brief summary of the accomplishments and conclusions of our work. The second part consists of two manuscripts, one being a paper presented at the 1998 MSAD Fluid Physics workshop, and the other to appear in *Physics of Fluids.*

1.2 Project Objectives

The objectives of our project were, first of all, to determine the accuracy of the Burnett constitutive equations for gases as applied to highly nonisothermal, slow-moving gases by comparison 'numerical experiments' provided by direct simulation monte carlo (DSMC) methods. Secondly, we were to use these findings to assess the feasibility of using the microgravity environment to experimentally isolate and measure the flows resulting from thermal stress (as predicted by the Burnett equations) in highly nonisothermal, buoyancy-free gases.

2 Technical Summary of the Project

2.1 Background and Motivation

The continuum description of momentum and energy transport in gases, based upon Newton–Stokes– Fourier constitutive relations, can become inaccurate in rarefied or highly nonequilbrium regimes, i.e., regimes in which the Knudsen number Kn ($= \lambda/L$, where λ is the gas mean free path and L is the characteristic system or gradient length) is no longer small. The Burnett equations, which represent the order–Kn^2 solution to the Boltzmann equation, ostensibly provide a means of extending continuum formulations into the transitional Knudsen regimes ($\sim Kn < 0.1$). The accuracy and validity of the Burnett equations, however, have not been firmly established. As has been noted by several authors, the asymptotic series expansion of the molecular distribution function – from which the Burnett equations are derived – has unknown convergence properties for finite Kn. The Burnett

equations can also lead to Second–law impossibilities, such as heat flux in an isothermal gas. Furthermore, the Burnett equations increase the order of the differential equations that govern momentum and heat transport in the gas. Additional boundary condition information is required to fully close the problem – yet such information is generally not available from physical principles alone.

Because of these issues, it is generally held that the Burnett equations are valid only in regimes in which the Navier-Stokes-Fourier level of approximation already provides an adequate description of transport, i.e., regimes in which the Burnett contributions represent a small perturbation to heat and momentum transport. Such conditions can be representative of high–Mach number flows, for which application of the Burnett equations appears to have been the most successful. On the other hand, there is not a broad understanding of the accuracy of the Burnett equations when applied to slow–moving, nonisothermal flow conditions. In principle, 'thermal stresses' (fluid stresses resulting from temperature gradients – which are predicted by the Burnett equations) could become a significant convection mechanism in buoyancy–free, nonisothermal gases. Indeed, it has been recently suggested that thermal stress convection could affect the growth of crystals in microgravity physical vapor transport experiments.

The project described here consisted of a theoretical and numerical examination of thermally–induced stresses and flows in enclosed, highly nonisothermal gases under buoyancy–free conditions. A central objective has been to identify a strategy in which stress and/or convection effects, as predicted by the Burnett equations, could be isolated and measured in microgravity–based experiments. Because of the questionable veracity of the Burnett equations, a second objective has been to test Burnett predictions of nonisothermal gas stress and convection with the exact description provided by the direct simulation Monte Carlo (DSMC) method.

2.2 Thermal stress in two–dimensional gases

The initial phase of the project was aimed at calculation, using continuum and DSMC methods, of gas convection in two dimensional nonuniformly heated rectangular enclosures. Typically, two adjacent surfaces of the enclosure were modeled as adiabatic, zero–stress surfaces (i.e., planes of symmetry), and the other two adjacent surfaces were maintained at specified temperature distributions with one surface transferring a net amount of heat

to the gas, and the other transferring the heat from the gas. According to continuum theory, convection in the enclosure would result from thermal stress in the bulk gas and thermal creep along the side walls – the latter mechanism being the slip flow of gas over a solid surface that is driven by a gas temperature gradient tangential to the surface.

Our continuum and DSMC calculations to date have not identified conditions in the enclosure that lead to measurable thermal stress flows that are comparable to or larger than thermal creep flows, and simultaneously maintain the $Kn < 0.1$ regime required of the Burnett equations. With the exception of the pure continuum limit ($Kn \rightarrow 0$, under which thermal stress vanishes), elimination of thermal creep cannot be accomplished by maintaining the heated/cooled walls at uniform temperatures. Rather, the discontinuity (or jump) between the surface and adjacent gas temperatures – which will be proportional to Kn and the local normal temperature gradient – will lead to nonuniform gas temperatures along the nonuniformly heated surfaces. For all realistic values of Kn, thermal creep flows generated by the temperature jump effects were substantially larger than those resulting from thermal stress.

To minimize the effects of creep, we performed additional simulations in which the temperature distributions along the heated/cooled surfaces were assigned to provide, for a given Kn, nearly uniform gas temperature adjacent to the surface. Surface temperature distributions were determined from solution of the gas conduction equation with uniform gas temperature boundary conditions along the adjacent heated/cooled surfaces, and subsequent application of the solution into the order$-Kn$ temperature jump relations. This approach imposed a surface temperature variation along the heated wall which increased towards the junction with the cooled wall, with an opposite trend along the cooled wall. The effect of this strategy largely eliminated thermal creep from continuum–based models. and left a computed flow field which was driven almost entirely by thermal stress. However, this strategy would also lead to highly nonequilibrium conditions in the vicinity of the hot/cold surface junction, for which the Burnett equations are not expected to hold. DSMC calculations on the same system showed convective flows that were qualitatively similar yet substantially larger than those predicted by the continuum model – even though the DSMC and continuum–calculated temperature fields were in significant agreement.

2.3 Thermal stress in one–dimensional gases

A more direct method of examining thermal stress effects would be to directly measure the normal stress in a gas that is contained between two parallel surfaces at different yet uniform temperature – which will eliminate convection from thermal creep. We have investigated the effects of thermal stress, as predicted by the Burnett equation, on the pressure distributions and normal stress in a stationary, buoyancy–free, hard–sphere gas for the case of one–dimensional heat transfer. Using First–Law principles and the Burnett equation, it can be shown that thermal stress results in a reduction in normal stress in the nonisothermal gas relative to that in the equilibrium state. The normal stress, in turn, can be obtained as an eigenvalue to a second–order ordinary differential equation, representing the Burnett equation, for the pressure distribution in the gas. Boundary conditions for the pressure at the heated and cooled surfaces can be obtained by an asymptotic expansion of the Burnett equations within the Knudsen rarefaction layers adjacent to the surfaces, which provides an order–Kn^2 correction the order–Kn pressure slip relations that are obtained from solution of the linearized Boltzmann equation at the gas/surface interface.

The Burnett and DSMC predictions of pressure are in close agreement for effective Knudsen numbers (based on the temperature gradient in the gas) less than 0.1. In particular, the Burnett equations can accurately describe the shape of the Knudsen (or rarefaction) layers adjacent to the heated and cooled surfaces that bound the gas, and can also describe the variation in pressure in the 'bulk' gas (i.e., outside the Knudsen layers). In addition, theoretical predictions of the reduction in normal stress correspond well to DSMC–derived values.

2.4 Conclusions

2.4.1 Validity of the Burnett equations

The original project was motivated by the concept of a slow–moving, nonisothermal gas flow driven entirely by thermal stress within the gas. Since buoyant forces would typically overwhelm the thermal stress forces in normal gravity conditions, we hypothesized, in the original proposal, that thermal stress flows could be realized under microgravity conditions. The central objective of the project was to conduct numerical simulations to determine 1) the validity of the Burnett equations as applied to slow–moving thermal

stress flows, and 2) ascertain the feasibility of using the microgravity environment to experimentally measure such flows.

Regarding objective 1) above, we were successful in demonstrating that the Burnett equations are consistent with DSMC 'reality' for the simple case of a 1–D, stationary nonisothermal gas. On the other hand, we obtained decidedly ambiguous results on the validity of the Burnett equations applied to 2–D nonisothermal, slow–moving gases. For such situations, DSMC results are only qualitatively similar to that predicted by the continuum–based Burnett model.

A problem with the 2–D simulations – which we were not able to overcome – was that the creation of wall heating conditions necessary to drive thermal stress flows (as predicted by the Burnett equations) lead to local Knudsen conditions that were outside of the range of validity of the Burnett equations. In principle, this could be alleviated by reducing the overall Knudsen conditions of the simulation to the near–continuum level (i.e., $Kn \ll 1$) – yet it is currently not feasible to simulate such conditions with DSMC. Specifically, the near–continuum case would require a very large set of computational molecules (since the 2–D DSMC method scales as $1/Kn^2$), and the very slow moving thermal stress flow in the near–continuum limit would be extremely difficult to resolve with DSMC statistics.

2.4.2 Role of microgravity

Microgravity conditions would not be needed to examine experimentally the effect of thermal stress on normal stress in 1–D, stationary nonisothermal gases. The hydrostatic pressure gradient would be insignificant under the $Kn \sim 0.1$ conditions necessary to resolve thermal stress effects.

Because of the inability of current DSMC methods to model near–continuum flows, we do continue to see a potential for using microgravity to examine the validity of the Burnett equations applied to 2–D nonisothermal gases.

3 Project Accomplishments

3.1 Graduate students

Mr. Rong Wei (MS, 1999) performed DSMC and continuum calculations of hard–sphere gas heat transfer and fluid flow in two–dimensional, rectangular

enclosures. His thesis examined the extent to which the Navier–Stokes–Fourier formulation of transport, with slip and jump corrected boundary conditions, could model heat transfer in rarefied gases with two–dimensional temperature profiles.

Mr. Joseph Ragan (MS) is currently working on the simulation of gas flow over heated surfaces that have directionally–dependent molecular accommodation properties. He was partially supported by the project for the first two quarters of 1999, and has recently received fellowship support from the National Defense Science and Engineering Grant program.

3.2 Publications and Presentations

1. "Drag and torque on N–aggregated spheres in creeping flow," A. V. Filippov, D. W. Mackowski, and D. E. Rosner, to be presented at the *AIChE* 1999 Annual Meeting.

2. Mackowski, D. W., Papdopoulos, D. H., and Rosner, D. E., "Comparison of Burnett and DSMC prediction of pressure distribution and normal stress in one dimensional, strongly nonisothermal gases," *Physics of Fluids*, to appear (1999).

3. "Modelling of heat and mass transfer in rarefied, highly–nonequilibrium conditions," Invited seminar, Mechanical Engineering Department, University of Alabama at Birmingham, May 1999.

4. "Investigation of thermal stress convection in nonisothermal gases under microgravity conditions," presented at the 1998 MSAD Fluid Physics workshop, Cleveland, OH.

5. "Modelling of heat and mass transfer in rarefied, highly–nonequilibrium conditions," Invited seminar, Mechanical Engineering Department, Michigan State University, November 1997.

INVESTIGATION OF THERMAL STRESS CONVECTION IN NONISOTHERMAL GASES UNDER MICROGRAVITY CONDITIONS

Daniel W. Mackowski, Mechanical Engineering Department
Auburn University, AL 36849. dmckwski@eng.auburn.edu

1. INTRODUCTION

The continuum description of momentum and energy transport in gases, based upon Newton–Stokes–Fourier constitutive relations, can become inaccurate in rarefied or highly nonequilbrium regimes, i.e., regimes in which the Knudsen number Kn ($= \lambda/L$, where λ is the gas mean free path and L is the characteristic system or gradient length) is no longer small. The Burnett equations, which represent the order–Kn^2 solution to the Boltzmann equation, ostensibly provide a means of extending continuum formulations into the transitional Knudsen regimes ($\sim Kn < 1$).

The accuracy and validity of the Burnett equations, however, have not been firmly established. As has been noted by several authors, the asymptotic series expansion of the molecular distribution function – from which the Burnett equations are derived – has unknown convergence properties for finite Kn.[1,2] The Burnett equations can also lead to Second–law impossibilities, such as heat flux in an isothermal gas.[3] Furthermore, the Burnett equations increase the order of the differential equations that govern momentum and heat transport in the gas. Additional boundary condition information is required to fully close the problem – yet such information is generally not available from physical principles alone.

Because of these issues, it is generally held that the Burnett equations are valid only in regimes in which the Navier-Stokes-Fourier level of approximation already provides an adequate description of transport, i.e., regimes in which the Burnett contributions represent a small perturbation to heat and momentum transport. Such conditions can be representative of high–Mach number flows, for which application of the Burnett equations appears to have been the most successful.[4–7] On the other hand, there is not a broad understanding of the accuracy of the Burnett equations when applied to slow–moving, nonisothermal flow (SNIF) conditions. As noted by Kogan, 'thermal stresses' (fluid stresses resulting from temperature gradients – which are predicted by the Burnett equations) could become a significant convection mechanism in buoyancy–free, nonisothermal gases.[8,9] Indeed, it has been recently suggested that thermal stress convection could affect the growth of crystals in microgravity physical vapor transport experiments.[10,11]

The work presented here consists of a theoretical and numerical examination of thermally–induced stresses and flows in enclosed, highly nonisothermal gases under buoyancy–free conditions. A central objective has been to identify a strategy in which stress and/or convection effects, as predicted by the Burnett equations, could be isolated and measured in microgravity–based experiments. Because of the questionable veracity of the Burnett equations, a second objective has been to test Burnett predictions of nonisothermal gas stress and convection with the exact description provided by the direct simulation Monte Carlo (DSMC) method.

2. PREDICTION OF THERMAL STRESS CONVECTION

The initial phase of the project was aimed at calculation, using continuum and DSMC methods, of gas convection in two dimensional nonuniformly heated rectangular enclosures. Typically, two adjacent surfaces of the enclosure were modeled as adiabatic, zero–stress surfaces (i.e., planes of symmetry), and the other two adjacent surfaces were maintained at specified temperature distributions with one surface transferring a net amount of heat to the gas, and the other transferring the heat from the gas.

The continuum formulations of momentum and energy transport are identical to Navier–Stokes–Fourier models, with the exception of the Burnett stress tensor in the momentum equations and the creep and jump boundary conditions. For the conditions examined here (i.e., slow–moving flow, with $Re_L \ll 1$) the only significant terms in the Burnett stress tensor relations will be those involving temperature gradients. This thermal stress component appears as[8,11]

$$\boldsymbol{\tau}_T = -\frac{\mu^2 \mathcal{R}}{P}\left[\omega_3\left(\nabla\nabla T - \frac{1}{3}(\nabla^2 T)\,\mathbf{I}\right) + \frac{\omega_5}{2T}\left((\nabla T)(\nabla T) - \frac{1}{3}(\nabla T\cdot\nabla T)\,\mathbf{I}\right)\right] \quad (1)$$

in which μ is the dynamic viscosity, R is the gas constant, and ω_3 and ω_5 are dimensionless, order–unity coefficients which depend on the interaction potential of the molecules. The creep and jump boundary conditions appear

$$\mathbf{u} = \frac{c_S \mu R}{P}\left(\nabla T - \hat{n}\,\frac{\partial T}{\partial n}\right) \quad (2)$$

$$T = T_w + \frac{c_T \lambda}{T}\,\frac{\partial T}{\partial n} \quad (3)$$

where n is the outward normal and the dimensionless coefficients c_S and c_T depend on the thermal and momentum accommodation properties of the surface.[12] Numerical solution of the governing equations was accomplished using the SIMPLER algorithm of Patankar.[13] Coefficients corresponding to hard−sphere molecules, which gives a temperature−dependent viscosity of $\mu \sim T^{1/2}$, were used in the computations.

Direct simulation Monte Carlo calculations of hard−sphere gas convection and heat transfer were accomplished using the standard procedure developed by Bird.[14,15] The cell size was nominally set to $0.1\lambda_0$, where λ_0 represents the mean−free−path at the equilibrium state of the system, and 10−20 molecules were assigned per cell. Simulations were conducted for a Knudsen range of $Kn = 0.01 - 0.2$. Because thermal creep and stress flows will be on the order of Kn times the mean molecular velocity, resolution of the flows using DSMC required simulation times on the order of 10^6-10^7 time steps.

Our continuum and DSMC calculations to date indicate that it would be very difficult to create conditions in the enclosure that result in measurable thermal stress flows that are comparable to or larger than thermal creep flows, and simultaneously maintain the $Kn < 0.1$ regime required of the Burnett equations. With the exception of the pure continuum limit ($Kn \to 0$, under which thermal stress vanishes), elimination of thermal creep cannot be accomplished by maintaining the heated/cooled walls at uniform temperatures. Rather, the discontinuity (or jump) between the surface and adjacent gas temperatures − which will be proportional to Kn and the local normal temperature gradient − will lead to nonuniform gas temperatures along the nonuniformly heated surfaces. For all realistic values of Kn, thermal creep flows generated by the temperature jump effects were substantially larger than those resulting from thermal stress.

To minimize the effects of creep, we performed additional simulations in which the temperature distributions along the heated/cooled surfaces were assigned to provide, for a given Kn, nearly uniform gas temperature adjacent to the surface. Surface temperature distributions were determined from solution of the gas conduction equation with uniform gas temperature boundary conditions along the heated/cooled surfaces, and subsequent application of the solution into Eq. (3) to predict $T_w(x)$. This approach imposed a surface temperature on the heated surface which increased towards the junction with the cooled surface, with an opposite trend along the cooled wall. The effect of this strategy resulted in thermal creep flows that were confined about the hot/cold junction, and left a bulk, thermal−stress driven convection pattern in the bulk of the enclosure. However, this strategy would also lead to highly nonequilibrium conditions in the vicinity of the hot/cold surface junction, for which the Burnett equations are not expected to hold.

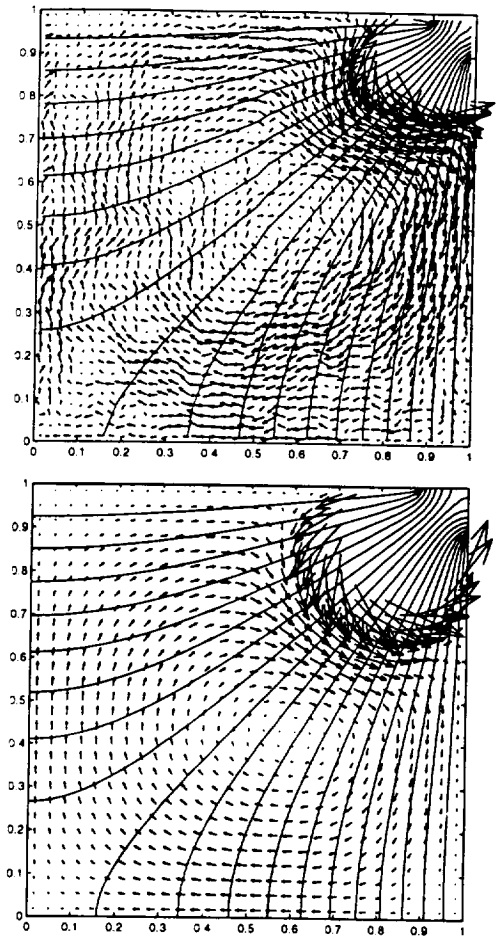

Fig. 1: DSMC (top) and continuum (bottom) results

The comparison between continuum/Burnett and DSMC predictions of convective flows in the enclosure has been inconclusive. DSMC calculations have shown convective flows that are qualitatively similar than those predicted by the continuum model. As an example, we show in Fig. 1 plots of velocity vectors and isotherms, calculated using the DSMC (top) and continuum (bottom) models, for a $Kn = 0.02$ hard−sphere gas contained in an enclosure with a relative temperature difference on the hot and cold walls of $2(T_H - T_C)/(T_H + T_C) = 1$. The heated wall is on the top, and the left and bottom walls are symmetry surfaces. A strip of the walls adjacent to the hot/cold junction, equal to 0.1 of the wall length, is held adiabatic, and the remainder of the walls have temperature distributions set to give isothermal gas conditions per the procedure discussed above. Velocity vectors corresponding to ther-

mal creep along the adiabatic surfaces (seen in the tight counterclockwise rotation in the upper right corner) have been removed from the plot to allow resolution of the thermal stress flows. The stress flow – as predicted by the continuum model – results in a clockwise rotation in the main body of the gas for the given conditions. A similar pattern is seen in the DSMC results. We cannot establish, however, whether the observed DSMC flows result from thermal stress, or are due to slip effects at the walls. As mentioned above, the veracity of the Burnett relations is also questionable for the highly nonequilibrium conditions of the simulations. On the other hand, temperature profiles calculated via DSMC and continuum models show significant agreement.

3. THERMAL STRESS IN 1-D HEAT TRANSFER

A simpler situation in which to compare continuum/Burnett and DSMC predictions of thermal stress effects is offered by 1–D heat transfer in a stationary gas. In this situation, the effects of thermal stress would be seen in the pressure distribution and normal stress in the gas.[16]

The computational domain was now taken to be a slab of gas contained between two parallel surfaces, separated by a distance L, with the surfaces at $x = 0$ and L maintained at uniform temperatures of T_{CS} and T_{HS} (with $T_{HS} > T_{CS}$), respectively. In nondimensional form (with pressure and stress normalized with the equilibrium pressure P_m and temperature by the equilibrium temperature T_m), the Burnett equation for the x–directed, normal component of the stress tensor is[7,17]

$$\tau^* = \phi + \frac{c_1 Kn^2 \theta}{\phi}\left[\omega_4 \frac{\theta'\phi'}{\phi} - \omega_2\left(\frac{\theta\phi'}{\phi}\right)' + \omega_3\theta'' + \omega_5\frac{\theta'^2}{\theta}\right] \qquad (4)$$

In the above, $\phi = P/P_m$, $\tau^* = \tau/P_m$, $\theta = T/T_m$, the prime denotes differentiation with respect to $\xi = x/L$, $c_1 = (4\pi/3)(5/16)^2 = 0.4091$, and the dimensionless ω coefficients depend on the molecular interaction potential. Since the gas is stationary and buoyancy–free, the stress τ will be a constant. In the limit of $Kn \to 0$, this gives the Navier–Stokes result of $P = \tau =$ constant. For finite Kn, however, the additional source of thermal stress can act within the nonisothermal gas. The magnitude of the thermal stress will vary with position – by virtue of the dependence of temperature and temperature gradient on position – and consequently pressure will vary to maintain a constant normal stress.

The Burnett equations make no contribution to the heat flux for a stationary gas. Consequently, the gas temperature will be described by

$$q^* = \text{constant} = \theta^{1/2}\theta' \qquad (5)$$

where q^* is the dimensionless heat flux ($= qL/kT_m$). Equation (5) can be used to combine the last two terms in Eq. (4), which results in

$$\tau^* = \phi + \frac{c_1 Kn^2}{\phi}\left[\theta\left(\omega_4\frac{\theta'\phi'}{\phi} - \omega_2\left(\frac{\theta\phi'}{\phi}\right)'\right) - \frac{c_2 q^{*2}}{\theta}\right] \qquad (6)$$

where $c_2 = (\omega_3 - 2\omega_5)/2 = 0.9900$ for hard–sphere molecules.

Two separate effects – or regimes – on ϕ can be anticipated from inspection of Eq. (6). One effect, which is discussed by Kogan[18] and Makashev[19], derives from the fact that the derivatives of ϕ will be multiplied by the small parameter (for near–continuum conditions) of Kn^2. The solution to Eq. (6) could therefore exhibit 'boundary layers' of width $\Delta\xi \sim Kn$. It is shown below that this property, combined with appropriate boundary conditions, will allow for a limited description of the Knudsen layers adjacent to the surfaces.

A second characteristic regime, as indicated by Eq. (6), would occur outside the Knudsen layers. By expanding ϕ in a power series of Kn^2, and neglecting all terms higher than Kn^2, the pressure distribution in the bulk gas would be given approximately by

$$\phi \approx \tau^* + \frac{c_1 c_2 (Kn\, q^*)^2}{\tau^* \theta} \qquad (7)$$

As is evident from inspection of Eq. (7), thermal stress would create a pressure gradient in the gas, with pressure increasing towards the cooler regions in the gas. The gradient would be proportional to the square of $Kn\, q^* \sim \sqrt{\theta}\, d\theta/d(x/\lambda)$ – which can be interpreted as a Knudsen number based on the characteristic length of the temperature gradient (note that this quantity is independent of L). It should be emphasized that the effect predicted from Eq. (7) is fundamentally different than the pressure gradient created by 'thermal transpiration' of a gas in a tube with an imposed axial temperature gradient.[20,21] The latter is a result of thermal slip at the walls of the tube, and leads to a pressure that increases in the direction of increasing temperature. Thermal stress, on the other hand, results from the effect of temperature gradients on the molecular velocity distribution function within the gas.

Although the thermal stress pressure gradient can be labeled 'hydrostatic' – since the gas is at rest – it

is distinctly different than that resulting from a gravitational acceleration in the $x-$direction. Unlike the latter, thermal stress would not result in a difference between the normal forces acting on the hot and cold surfaces. In other words, the 'pressure' measured at the surfaces – which would physically represent the normal stress τ – would be identical for both surfaces.

Thermal stress, however, will result in a different value of the normal stress than that predicted from the Navier–Stokes level of approximation. This follows from conservation of energy requirements. In particular, the average pressure in the gas represents the equilibrium pressure that would be attained if the walls were instantaneously made adiabatic. Since the equilibrium pressure is used to normalize the dimensional pressure P, this statement is equivalent to

$$\int_0^1 \phi \, d\xi = 1 \qquad (8)$$

Regardless of the values of q^* and Kn, the pressure distribution in the gas must satisfy the energy conservation constraint implied by Eq. (8). Consequently, the normal stress τ^* would be obtained as the eigenvalue to Eq. (6) such that the solution (for specified boundary conditions) satisfies Eq. (8). In general, this value will be different than the Navier–Stokes result of $\tau^* = 1$.

An approximate value for τ^* can be obtained by neglecting the effects of the Knudsen layers at the surfaces, for which the pressure distribution would be given by Eq. (7). To order Kn^2, this gives[16]

$$\tau^* \approx 1 - c_1 c_2 \left(Kn\, q^*\right)^2 \qquad (9)$$

This relatively–simple approximation indicates that thermal stress will lower the normal stress in a closed system relative to that predicted from the Navier–Stokes level – although we note again that the effects of Knudsen layers have been neglected in the analysis.

The final elements required to close the problem are the boundary conditions for pressure. As is the case with the Navier–Stokes approximation, the boundary conditions for the Burnett equations should represent an extrapolation of the solution across the region, adjacent to the wall, where the solution is no longer valid. Makashev[19] and Schamberg[22] have proposed boundary conditions that are consistent with the order–Kn^2 accuracy of the Burnett equations. The accuracy of these approaches, however, has not been well established.[23] Alternatively, order–Kn relations can be derived for the pressure 'slip' adjacent to a heated or cooled surface.[12,21] However, our work at this stage is primarily concerned with determining whether there are boundary conditions which, when coupled to the

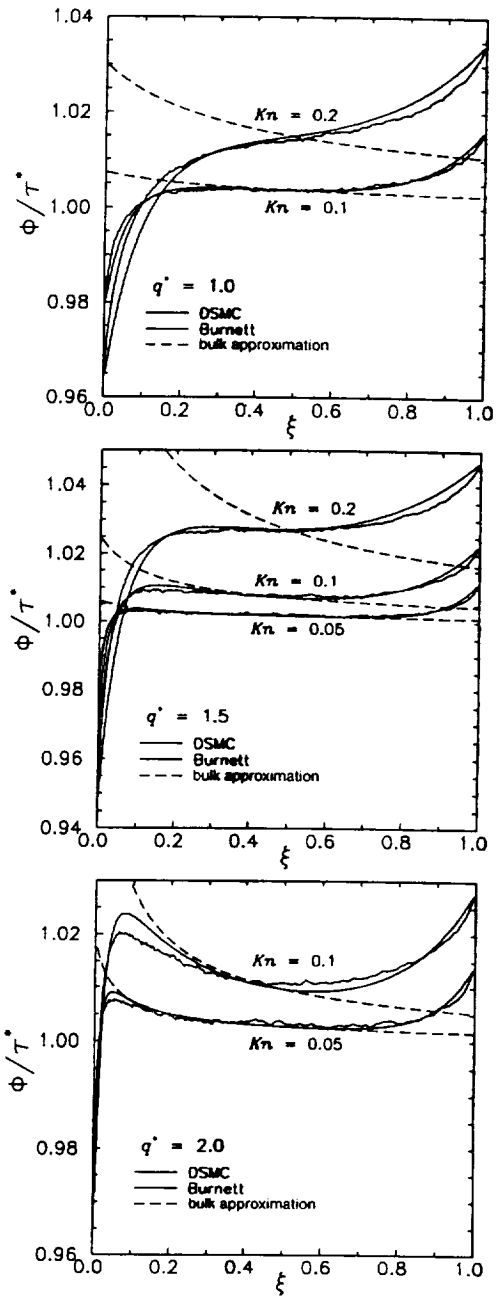

Figs. 2–4: DSMC and continuum pressure distributions

Burnett equations, can reproduce DSMC predictions of pressure distributions in a nonisothermal gas. Therefore, the pressures at the hot and cold surfaces were taken to be parameters, and were chosen to provide the best agreement between theory and DSMC results. The obvious choice for the pressure at the surfaces will be the values determined from DSMC predictions.

Comparisons of Burnett (via numerical solution of Eq. (6)) and DSMC predictions of pressure distribution appear in Figs. 2–4. Each plot shows $P/\tau = \phi/\tau^*$ vs.

$xi = x/L$ for a fixed value of q^*, with Kn a parameter. Two theoretical predictions of P/τ are shown for each set of DSMC results. The first corresponds to the numerical solution of Eq. (6), with boundary conditions obtained from extrapolation of the DSMC–derived pressures to the surfaces and temperatures predicted from Eq. (5). The second represents the bulk gas thermal stress pressure distribution predicted from Eq. (7), which does not account for boundary effects. This latter prediction has been shifted by a constant to match with the full–Burnett solution at $\xi = 0.5$.

As is evident from the results, the pressure profiles show distinct Knudsen layers at both the cooled and heated surfaces. The drop in pressure at the cooled surface, and the increase in pressure at the hot surface, are both consistent with the predictions of pressure slip relations.[21] The pressure drop at the cold surface can be considerable for the conditions examined here – amounting to around an 8% decrease for $Kn = 0.2$ and $q^* = 1.5$.

The solutions of the Burnett equation, with DSMC derived boundary conditions, are seen to capture the essential features of the DSMC pressure distribution. In particular, the solutions provide a good description of the width and form of the Knudsen layers and the pressure distribution outside the layers. The difference between the theoretical and DSMC results is greatest at the edge of the cold–surface Knudsen layers, for which the theoretical model tends to overpredict the pressure. This is most evident for the results corresponding to $q^* = 2.0$ in Fig. 4. Nevertheless, the fact that the Burnett equations can resolve, to a reasonable accuracy, the Knudsen layers at the surface is somewhat surprising – especially when considering that the theory is based on the order–Kn continuum temperature profile. We also examined solutions to Eq. (6) using boundary values of ϕ that were different than the DSMC results, and found that the exact, DSMC–derived boundary conditions provide the best overall agreement between Burnett equation predictions and DSMC results.

The DSMC results for $q^* = 2.0$ appear to show a pressure distribution in the bulk gas that is described by Eq. (7). On the other hand, the pressure distribution for $q^* = 1.5$ and $Kn = 0.2$ (Fig. 3) – for which Eq. (7) predicts a greater effect – is dominated by the Knudsen layers extending from the surfaces. To eliminate the effects of the Knudsen layers at the hot wall, we performed additional DSMC calculations in which the velocities of the incoming molecules at the hot boundary were sampled from the Chapman–Enskog distribution function for the fixed values of q^* and Kn. By doing so, the hot surface now approximated an open boundary. The corresponding DSMC results showed a

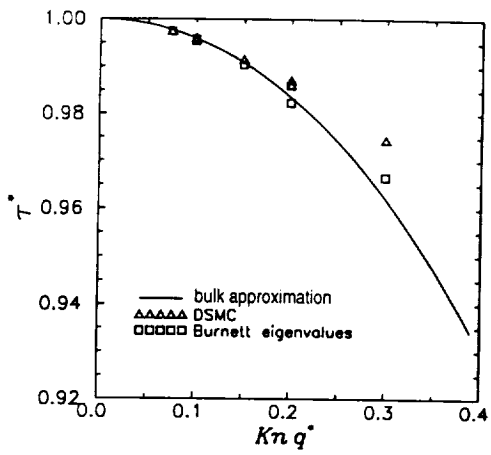

Fig. 5: DSMC and continuum normal stress

pressure distribution in the bulk gas that was accurately represented by Eq. (7).

A final comparison of theory and experiment can be obtained from the dimensionless normal stress. The simplified model of Eq. (9) indicates that τ^* should be a function primarily of $Kn\,q^*$. Accordingly, we plot in Fig. 5 the DSMC values of τ^* vs. $Kn\,q^*$ for the seven different combinations of Kn and q^* that were used in the closed system calculations (results of Figs. 2–4). Theoretical results correspond to the derived eigenvalues of Eq. (6) for the DSMC–derived boundary conditions, and to the approximation given by Eq. (9).

The first point to make is that the predictions of τ^* from full solution of the Burnett differential equation are nearly equivalent to those obtained from the bulk–gas approximation of Eq. (9). Evidently, the decrease in pressure at the cold surface is compensated by the increase at the hot, so that the Knudsen layers have a small effect on the averaged pressure in the gas. Secondly, the primary dependence of τ^* on $Kn\,q^*$ is supported in the DSMC results at $Kn\,q^* = 0.1$ and 0.2 – which each correspond to two combinations of Kn and q^*. As observed, the results are nearly identical at these points. Finally, the theoretical predictions are in excellent agreement with the DSMC results for $Kn\,q^* \leq 0.15$, beyond which the theory overpredicts the decrease in τ^*. As can be seen from the results, the relative decrease in normal stress on the surfaces is quite small, i.e., $\tau^* = 0.975$ for $q^* = 2.0$ and $Kn = 0.2$, or a 2.5% decrease in 'measured' pressure at the surface. We should emphasize, however, that this decrease is still significantly larger than the numerical precision of the DSMC simulations.

SUMMARY

The project has sought to ascertain the veracity of

the Burnett relations, as applied to slow moving, highly nonisothermal gases, by comparison of convection and stress predictions with those generated by the DSMC method. The Burnett equations were found to provide reasonable descriptions of the pressure distribution and normal stress in stationary gases with a 1–D temperature gradient. Continuum/Burnett predictions of thermal stress convection in 2–D heated enclosures, however, are not quantitatively supported by DSMC results. For such situations, it appears that thermal creep flows, generated at the boundaries of the enclosure, will be significantly larger than the flows resulting from thermal stress in the gas.

ACKNOWLEDGEMENTS

This work has been supported through NASA–MSAD contract NAG3–1882, R. Balasubramaniam, technical contract officer. The author has benefitted from helpful collaborations with Daniel Rosner and Dimitrios Papadopoulos.

REFERENCES

[1] S. Chapman, and T. G. Cowling, *The Mathematical Theory of Non-Uniform Gases* (Cambridge University Press, London, 1970).

[2] C. Cergignani, *Mathematical Methods in Kinetic Theory*, Second Edition (Plenum Press, New York, 1990), ch. 5.

[3] L. A. Woods, *An Introduction to the Kinetic Theory of Gases and Magnetoplasmas*, Oxford University Press, 1993.

[4] K. A. Fisko and D. R. Chapman, "Comparison of Burnett, Super--Burnett, and Monte--Carlo solutions for hypersonic shock structure," *Rarefied Gas Dynamics: Theoretical and Computational Techniques*, E. P. Muntz, D. P. Weaver, and D. H. Campbell, Eds., Vol. 118, Progress in Astronautics and Aeronautics, 1989, pp. 374--395.

[5] G. C. Pham--Van--Diep, D. A. Erwin, and E. P. Muntz, "Testing continuum descriptions of low--Mach--number shock structures," *J. Fluid Mech.* **232**, 403 (1991).

[6] F. E. Lumpkin and D. R. Chapman, "Accuracy of the Burnett equations for hypersonic real gas flows," *J. Thermophysics Heat Transfer* **6**, 419 (1992).

[7] X. Zhong, R. W. MacCormack, and D. R. Chapman, "Stabilization of the Burnett equations and application to hypersonic flows," *AIAA J.* **31**, 1036 (1993).

[8] M. N. Kogan, "Molecular Gas Dynamics," in *Annual Review of Fluid Mechanics*, M. Van Dyke and W. G. Vincenti, Eds., Annual Review, Palo Alto, 1973, Vol. 5, pp. 383.

[9] Y. Sone, "Flow induced by thermal stress in rarefied gas," *Phys. Fluids* **15**, 1418 (1972).

[10] D. E. Rosner, "Side wall gas 'creep' and 'thermal stress convection in microgravity experiments on film growth by vapor transport," *Phys. Fluids* **A1**, 1761 (1989).

[11] A. Viviani and R. Savino, "Recent developments in vapour crystal growth fluid dynamics," *J. Crystal Growth* **133**, 217 (1993).

[12] S. K. Loyalka, "Temperature jump and thermal creep slip: rigid sphere gas," *Phys. Fluids A* **1**, 403 (1989).

[13] S. V. Patankar, *Numerical Heat Transfer and Fluid Flow*, McGraw-Hill, N.Y., 1980.

[14] G. A. Bird, *Molecular Gas Dynamics and the Direct Simulation of Gas Flows*, (Oxford, Clarendon Press, 1994).

[15] D. H. Papadopoulos and D. E. Rosner, "Enclosure gas flows driven by non--isothermal walls," *Phys. Fluids* **7**, 2535 (1995).

[16] D. W. Mackowski, D. H. Papadopoulos, and D. E. Rosner, 'Comparison of Burnett and DSMC preditions of pressure distributions and normal stress in one--dimensional, strongly nonisothermal gases," *Phys. Fluids*, in review (1998).

[17] C. J. Lee, "Unique determination of solutions to the Burnett equations," *AIAA J.* **32**, 985 (1994).

[18] M. N. Kogan, *Rarefied Gas Dynamics* (Plenum Press, New York, 1969), ch. 3.

[19] N. K. Makashev, "On the boundary conditions for the equations of gas dynamics corresponding to the higher approximations in the Chapman--Enskog method of solution of the Boltzmann equation," *Fluid Dyn.* **14**, 385 (1979).

[20] J. C. Maxwell, "On the stresses in rarefied gases arising from inequalities of temperature (appendix)," *Philos. Trans. Roy. Soc. Lond.* **170**, 231 (1979).

[21] D. C. Wadsworth, "Slip effects in a confined rarefied gas. I: temperature slip," *Phys. Fluids A* **5**, 1831 (1993).

[22] R. Schamberg, "The fundamental difference equations and the boundary conditions for high speed slip flow," Ph.D. Thesis, California Inst. Tech., Pasadena, CA, 1947.

[23] X. Zhong and K. Koura, "Comparison of solutions of the Burnett equations, Navier--Stokes equations, and DSMC for Couette flow," *Twentieth International Symposium on Rarefied Gas Dynamics*, Bejing, 1996.

Comparison of Burnett and DSMC Predictions of Pressure Distributions and Normal Stress in One–Dimensional, Strongly Nonisothermal Gases[†]

Daniel W. Mackowski*, Department of Mechanical Engineering,
Auburn University, Auburn, AL, 36849, USA

Dimitrios H. Papadopoulos and Daniel E. Rosner, Department of Chemical Engineering,
Yale University, New Haven, CT, 06520, USA

* Corresponding author: (334) 844–3334, (334) 844-3307 (FAX),
dmckwski@eng.auburn.edu

PACS numbers: 47.11+j, 47.45.-n, 47.70.Nd

[†] *Physics of Fluids*, 1999 (in press)

The Burnett equations have been shown to provide improved descriptions, relative to the Navier–Stokes equations, of flow structure in high–velocity (i.e., hypersonic) gases. We examine here the accuracy of the Burnett constitutive equation for fluid stress as applied to stationary gases. Specifically, we investigate the effects of 'thermal stress' (fluid stress induced by a temperature gradient), as predicted by the Burnett equation, on the pressure distributions and normal stress in a stationary, buoyancy–free, hard–sphere gas for the case of one–dimensional heat transfer. We show, using First–Law principles and the Burnett equation, that thermal stress results in a reduction in normal stress in the nonisothermal gas relative to that in the equilibrium state. The normal stress, in turn, can be obtained as an eigenvalue to a second–order ordinary differential equation, representing the Burnett equation, for the pressure distribution in the gas. Simple asymptotic solutions to the Burnett equation are developed, and are used in combination with order–Kn pressure slip relations to formulate pressure boundary conditions at the heated and cooled surfaces. The approximate solutions, as well as exact numerical calculations, are compared with pressure distributions generated from the direct–simulation–Monte–Carlo (DSMC) method. The Burnett and DSMC predictions of pressure are in good agreement for effective Knudsen numbers (based on the temperature gradient in the gas) less than 0.1. In particular, the Burnett equations can provide a reasonable description of the Knudsen (or rarefaction) layers adjacent to the heated and cooled surfaces that bound the gas, and can also describe the variation in pressure in the bulk gas. In addition, theoretical predictions of the reduction in normal stress correspond well to DSMC–derived values.

I. BACKGROUND AND MOTIVATION

In 1938. Burnett developed an approximate solution to the Boltzmann equation, based upon the asymptotic expansion procedure of Chapman and Enskog, that provided constitutive relations accurate to order Kn^2 (where $Kn = \lambda/L$ is the Knudsen number, with λ and L the mean free path and characteristic system length).[1,2] Ostensibly, these relations, commonly referred to as the Burnett equations, offered a means of extending continuum–based descriptions of momentum and heat transport in a gas to transitional Knudsen regimes. However, the accuracy and validity of the Burnett equations have not been firmly established. As has been noted by several authors, the asymptotic series expansion of the molecular distribution function – from which the Burnett equations are derived – has unknown convergence properties for finite Kn.[2,3] Furthermore, the Burnett equations increase the order of the differential equations that govern momentum and heat transport in the gas. Additional boundary condition information is required to fully close the problem – yet such information is generally not available from physical principles alone. Lee[4] has recently shown that, as expected, the lack of higher–order boundary conditions, coupled with the Burnett equations, can result in non–unique solutions of velocity, temperature, and pressure in steady Couette flow. The Burnett equations can also lead to Second–Law impossibilities in certain situations, such as a negative dissipation function or a heat flux in an isothermal gas.[5,6]

Because of these issues, it is generally held that the Burnett equations are valid only in regimes in which the Navier–Stokes–Fourier level of approximation already provides an adequate description of transport, i.e., regimes in which the Burnett contributions represent a small perturbation to heat and momentum transport. Such conditions can be representative of high–Mach number flows, for which application of the Burnett equations appears to have been the most successful.[7–10] On the other hand, there is not a broad understanding of the accuracy of the Burnett equations when applied to slow–moving, nonisothermal flow conditions. As noted by Kogan, 'thermal stresses' (fluid stresses resulting from temperature gradients – which are predicted by the Burnett equations) could become a significant convection mechanism in buoyancy–free, nonisothermal gases.[11,12] Indeed, it has been recently recognized that thermal stress convection could affect the growth of crystals in highly–nonisothermal yet buoyancy–free microgravity physical vapor transport experiments.[13,14]

An estimation of the characteristic thermal stress velocity in slow–moving, nonisothermal flow conditions can be obtained from an order–of–magnitude analysis of the Burnett

equations, which yields[14]

$$V_{TS} \approx \frac{\nu}{L}\left(\frac{\Delta T}{T}\right)^3$$

where ν is the gas kinematic viscosity, and T and ΔT are the characteristic system temperature and temperature difference, respectively. Assuming $(\Delta T)/T \sim 1$, the thermal stress velocity will be on the order of the momentum diffusion velocity – which corresponds to order–unity Reynolds flows. Such 'creeping' flows would, in principle, represent a small perturbation from the zero velocity and constant pressure conditions that would be trivially predicted by the Navier–Stokes equations (with no–slip boundary conditions). Yet by this very reasoning, the presence of flows and pressure gradients in a nonisothermal, buoyancy–free gas would be an unambiguous indication of the effects of thermal stress.

The objective of this paper is to, first of all, apply the Burnett equations to the situation of one–dimensional heat transfer in a quiescent gas, and theoretically predict the pressure distribution that is induced in the gas from thermal stress. Secondly, we will employ the 'numerical experiment' provided by the direct simulation Monte Carlo (DSMC) method, applied to the same system, to ascertain the accuracy of the Burnett equation predictions. We focus on pressure effects in a 1–D, stationary, nonisothermal gas in the absence of gravity, as opposed to 2–D gas motion induced by thermal stress, primarily because the weak, order–Kn^2 convection predicted by the Burnett equations would be difficult to resolve with DSMC statistics. In addition, a 2–D nonisothermal configuration would result in gas convection from thermal slip at the boundaries, which would interfere with our intention of isolating the effects of thermal stress.[15,16]

Investigations along the same lines as those conducted here have been recently performed by Wadsworth[17] and Zhong and Koura[18], who used DSMC to examine the accuracy of continuum formulations (Navier–Stokes with or without the Burnett terms) for 1–D heat transfer. In all previous examinations of which we are aware, the ability of the Burnett equations to predict pressure distributions in a quiescent, non–isothermal gas has not been addressed. One reason why this effect has escaped scrutiny, as will be shown below, is that it is essentially negligible under moderately nonisothermal and near–continuum (e.g., $Kn < 0.1$) conditions. A second reason has been the lack of well–established boundary conditions for pressure at a heated/cooled surface (i.e., pressure slip) which are consistent with the order–Kn^2 accuracy of the Burnett equations. Our approach to this latter point will be to develop, via a simple asymptotic analysis of the Burnett stress equation in the Knudsen layer, a thermal stress correction to order–Kn pressure slip at the surfaces.

II. THEORETICAL FORMULATION

A. System Configuration and Problem Definition

The system, which is schematically illustrated in Fig. 1, consists of a stationary, hard-sphere monatomic gas that is contained between two parallel, infinite-area boundaries that are separated by a distance L. A heat flux of q is flowing in the gas in the negative x direction. The system is in steady-state, and gravity is absent.

To identify the relevant system parameters which affect the pressure distribution, we present our analysis in a nondimensional form. The nondimensional temperature, pressure, and position are defined

$$\theta = \frac{T}{T_{ref}}, \quad \phi = \frac{P}{P_{ref}}, \quad \xi = \frac{x}{L} \tag{1}$$

where T_{ref} and P_{ref} are an appropriate reference temperature and pressure, which are defined below. We use the viscosity-based mean free path to define the Knudsen number;

$$Kn = \frac{\lambda_{ref}}{L} = \frac{16\,\mu_{ref}}{5LP_{ref}} \left(\frac{RT_{ref}}{2\pi}\right)^{1/2} \tag{2}$$

where R is the specific gas constant and μ is the dynamic viscosity. The thermal conductivity k is given by $k = 15R\mu/4$, and both k and μ are proportional to $T^{1/2}$ for the hard-sphere gas. Finally, the nondimensional heat flux and normal fluid stress are defined as

$$q^* = \frac{qL}{k_{ref}T_{ref}}, \quad \tau^* = \frac{\tau}{P_{ref}} \tag{3}$$

B. Continuum Formulation

In nondimensional form, the Burnett equation for the x-directed, normal component of the stress tensor is[4,10]

$$\tau^* = \phi + \frac{c_1 Kn^2 \theta}{\phi}\left[\omega_4 \frac{\theta'\phi'}{\phi} - \omega_2\left(\frac{\theta\phi'}{\phi}\right)' + \omega_3\theta'' + \omega_5\frac{\theta'^2}{\theta}\right] \tag{4}$$

where the prime denotes differentiation with respect to ξ, $c_1 = (4\pi/3)(5/16)^2 = 0.4091$, and the dimensionless ω coefficients depend on the molecular interaction potential. For hard-sphere molecules, the values are

$$\omega_2 = 2.028, \quad \omega_3 = 2.418, \quad \omega_4 = 0.681, \quad \omega_5 = 0.219 \tag{5}$$

We include the hydrostatic pressure P into our definition of the normal stress solely for convenience. Since the gas is stationary and buoyancy-free, the stress τ will be a constant.

In the limit of $Kn \to 0$, this gives the Navier–Stokes result of $P = \tau =$ constant. For finite Kn, however, the additional source of thermal stress can act within the nonisothermal gas. The magnitude of the thermal stress will vary with position – by virtue of the dependence of temperature and temperature gradient on position – and consequently pressure will vary to maintain a constant normal stress.

The Burnett equations make no contribution to the heat flux for a stationary gas. Consequently, the gas temperature will be described by

$$q^* = \text{constant} = \theta^{1/2}\theta' \tag{6}$$

This is integrated from $\xi = 0$ (the cold surface) to yield

$$\theta = \left[\theta_C^{3/2} - \frac{3q^*\xi}{2}\right]^{2/3} \tag{7}$$

As is well recognized, the dimensionless temperature θ_C should not be interpreted as the actual gas temperature directly at the surface. Rather, it represents the extrapolation to the surface of the temperature distribution outside the Knudsen (or rarefaction) layer.[17,19,20] This 'apparent' gas surface temperature is related to the solid surface temperature, θ_{CS}, by a slip condition, which appears as

$$\theta_C = \theta_{CS}\left(1 + c_t\, Kn\, \theta'_{\xi\to 0}\right) \tag{8}$$

in which c_t is a constant. We use the value $c_t = 1.691$, which was derived by Loyalka by solution of the linearized Boltzmann equation for 1–D heat transfer in a hard–sphere gas and for perfectly accommodating surfaces.[19] By setting $\xi = 1$ in Eq. (7), the heat flux is related to the hot–side boundary temperature by

$$q^* = \frac{2}{3}\left(\theta_H^{3/2} - \theta_C^{3/2}\right) \tag{9}$$

The corresponding slip condition at the hot surface is

$$\theta_H = \theta_{HS}\left(1 - c_t\, Kn\, \theta'_{\xi\to 1}\right) \tag{10}$$

For reasons which will become apparent in a following section, we will now define the reference temperature T_{ref} so that

$$1 = \left(\int_0^1 \frac{d\xi}{\theta}\right)^{-1} = \frac{\theta_H^{3/2} - \theta_C^{3/2}}{3(\theta_H^{1/2} - \theta_C^{1/2})} \tag{11}$$

By combining Eqs. (9) and (11), θ_C and θ_H can be obtained as functions of q^*, i.e.,

$$\theta_C = \frac{1}{24}\left[24 + q^{*2} - \sqrt{3}\,q^*\left(48 - q^{*2}\right)^{1/2}\right] \tag{12}$$

Note that the maximum value of q^*, which corresponds to $\theta_C \to 0$, is $2\sqrt{3} = 3.464$.

Equation (6) can be used to combine the last two terms in Eq. (4), which results in

$$\tau^* = \phi + \frac{c_1 Kn^2}{\phi}\left[\theta\left(\omega_4\frac{\theta'\phi'}{\phi} - \omega_2\left(\frac{\theta\phi'}{\phi}\right)'\right) - \frac{c_2 q^{*2}}{\theta}\right] \tag{13}$$

where $c_2 = (\omega_3 - 2\omega_5)/2 = 0.9900$. Equation (13) provides a second-order, nonlinear ordinary differential equation for the pressure distribution in the gas. Complete solution requires specification of the nondimensional stress τ^* and a pair of boundary conditions for ϕ. Alternatively, the equation could be differentiated, which would eliminate τ^* yet add an additional boundary condition for ϕ – since the equation would become third order. We will work with the equation as it appears in Eq. (13), and employ thermodynamic principles to infer the value of τ^*. Our approach is discussed in the next section.

C. Characteristics of Thermal Stress and Boundary Conditions

Equation (13) displays the characteristic stiff form of the Burnett equations, in which the derivatives of the dependent variables (in this case ϕ) are multiplied by the small parameter Kn^2. Accordingly, the solution to Eq. (13) would be expected to display an inner (or boundary layer) regime, in which the derivatives of ϕ contribute to the solution, and an outer regime in which the derivatives have little effect. Kogan[21] and Makashev[22] have noted that this property of the Burnett equations, when combined with order-Kn^2 boundary conditions, would allow for a limited description of the Knudsen layers that occur at the surface/gas interfaces.

We will ultimately use a numerical solution to Eq. (13) to make quantitative comparisons between the Burnett and DSMC predictions of pressure distribution. However, insight into the effects of thermal stress on the pressure and normal stress in the gas – as well as a check of the consistency of the solution with regard to Kn constraints – can be obtained from relatively simple, order-Kn^2 asymptotic approximations to the inner and outer solution regimes to Eq. (13).

The outer regime is examined first. By expanding ϕ in a power series of Kn^2, and neglecting all terms higher than Kn^2, the pressure distribution in the bulk gas would be given approximately by

$$\phi \approx \tau^* + \frac{c_1 c_2 (Kn\,q^*)^2}{\tau^*\theta} \tag{14}$$

As is evident from inspection of Eq. (14), thermal stress would create a pressure gradient in the gas, with pressure increasing towards the cooler regions in the gas. The gradient would be proportional to the square of $Kn\, q^* \sim \sqrt{\theta}\, d\theta/d(x/\lambda)$ - which can be interpreted as a Knudsen number based on the characteristic length of the temperature gradient (note that this quantity is independent of L). Accordingly, the outer solution would be valid only for $Kn\, q^* \ll 1$. It should be emphasized that the effect predicted from Eq. (14) is fundamentally different than the pressure gradient created by 'thermal transpiration' of a gas in a tube with an imposed axial temperature gradient.[17,23] The latter is a result of thermal slip at the walls of the tube, and leads to a pressure that increases in the direction of increasing temperature. Thermal stress, on the other hand, results from the effect of temperature gradients on the molecular velocity distribution function within the gas.

Even though the thermal stress pressure gradient can be labeled 'hydrostatic' - since the gas is at rest - it is distinctly different than that resulting from a gravitational acceleration in the x-direction. Unlike the latter, thermal stress would not result in a difference between the normal forces acting on the hot and cold surfaces. In other words, the 'pressure' measured at the surfaces - which would physically represent the normal stress τ - would be identical for both surfaces.

Thermal stress, however, will result in a different value of the normal stress than that predicted from the Navier–Stokes level of approximation. This follows from conservation of energy requirements. In particular, the average pressure in the gas, given by

$$P_m = \frac{1}{L}\int_0^L P\, dx = \frac{R}{L}\int_0^L \rho T\, dx$$

represents the equilibrium pressure that would be attained if the walls were instantaneously made adiabatic. If the reference pressure is defined as $P_{ref} = P_m$, the above equation is equivalent to

$$\int_0^1 \phi\, d\xi = 1 \tag{15}$$

Regardless of the values of q^* and Kn, the pressure distribution in the gas must satisfy the energy conservation constraint implied by Eq. (15). Consequently, the normal stress τ^* would be obtained as the eigenvalue to Eq. (13) such that the solution (for specified boundary conditions) satisfies Eq. (15). In general, this value will be different than the Navier–Stokes result of $\tau^* = 1$.

An approximate value for τ^* can be obtained by neglecting the effects of the Knudsen layers at the surfaces, for which the pressure distribution would be given by the outer

solution of Eq. (14). Integration of this equation over ξ gives

$$\int_0^1 \phi \, d\xi = 1 \approx \tau^* + \frac{c_1 c_2 (Kn\, q^*)^2}{\tau^*} \int_0^1 \frac{d\xi}{\theta_m} = \tau^* + \frac{c_1 c_2 (Kn\, q^*)^2}{\tau^*} \tag{16}$$

where we have used the definition of the reference temperature per Eq. (11). Solving Eq. (16) for τ^* yields

$$\tau^* \approx \frac{1}{2}\left[1 + \left(1 - 4c_1 c_2 \left(Kn\, q^*\right)^2\right)^{1/2}\right] \tag{17}$$

which, to order Kn^2, is

$$\tau^* \approx 1 - c_1 c_2 \left(Kn\, q^*\right)^2 \tag{18}$$

This relatively-simple approximation indicates that thermal stress will lower the normal stress in a closed system relative to that predicted from the Navier–Stokes level - although we note again that the effects of Knudsen layers have been neglected in the analysis.

We turn now to an examination of the Knudsen layer region adjacent to the cold surface (an analysis at the hot surface would follow an analogous approach). Our objective here is to obtain a simple description of the boundary layer behavior predicted by Eq. (13). To do this, we assume that the Knudsen layer introduces an order–Kn perturbation in the pressure field - which is based the fact that pressure slip at a heated/cooled surface occurs at the order–Kn level.[17,19] Accordingly, the pressure distribution in the Knudsen layer is estimated by superimposing the average bulk effect, given by Eq. (14), with an order–Kn undetermined function f_1, via

$$\phi_{inner} = \tau^* + Kn\, f_1 + Kn^2\, b \tag{19}$$

in which $b = c_1 c_2 q^{*2}/(\tau^* \, \overline{\theta}_C)$, with $\overline{\theta}_C$ representing the average temperature in the Knudsen layer, i.e., the average from $\xi = 0$ to $\theta_C Kn$. We now replace this form into Eq. (13), substitute ξ with the stretched variable $\eta = \xi/Kn$, expand the equation in powers of Kn, and retain terms to order–Kn. This gives the simple differential equation

$$\frac{d^2 f_1}{d\eta^2} - a\, f_1 = 0 \tag{20}$$

where $a = \tau^{*2}/(c_1 \omega_2 \theta_C^2)$ is an order–unity constant. The surface boundary condition for pressure is assumed to be in a similar form as Eq. (19);

$$\phi(0) \equiv \phi_C = \tau^* + Kn\, f_{1C} + Kn^2\, b \tag{21}$$

and the outer boundary condition has $f_1 \to 0$ for $\eta \to \infty$. Upon solution of Eqs. (20) and (21), the inner pressure distribution approximation is

$$\phi_{inner} = \tau^* + Kn^2\, b + \left(\phi_C - \tau^* - Kn^2\, b\right) \exp\left[-\sqrt{a}\,\eta\right] \tag{22}$$

A composite solution, which approximates the pressure distribution in both the inner and outer regimes, is obtained by combining Eqs. (22) and (14), and adjusting the result by a constant to maintain the $\phi(0) = \phi_C$ condition. This results in

$$\phi \approx \tau^* + Kn^2\, b \left[1 + \bar{\theta}_C \left(\frac{1}{\theta(\xi)} - \frac{1}{\theta_C}\right)\right] + \left(\phi_C - \tau^* - Kn^2\, b\right) \exp\left(-\frac{\sqrt{a}}{Kn}\,\xi\right) \tag{23}$$

Since $1 - \bar{\theta}_C/\theta_C \sim O(Kn)$, the outer part of this approximation is consistent, to order Kn^2, to that in Eq. (14).

The boundary layer effect is observed, in this simplified analysis, in the exponential decay of pressure from the boundary to the freestream value. The characteristic width of the layer will be $\Delta\xi \approx Kn/\sqrt{a} \sim Kn\,\theta_C$, i.e., proportional to the local mean free path, as expected. In addition, the pressure gradient at the surface, which is approximated by

$$\left.\frac{d\phi}{d\xi}\right|_{\xi\to 0} \approx \left(\phi_C - \tau^*\right) \frac{\sqrt{a}}{Kn} + O(Kn^2)$$

is order unity since $\phi_C - \tau^*$ is order–Kn. Consequently, the solution maintains the constraint that $Kn\,\phi' \ll 1$ within the Knudsen layer, providing that $Kn \ll 1$.

The final elements required to close the problem – and allow for a quantitative comparison between the Burnett equation and DSMC predictions – are the boundary conditions for pressure. In formulating the problem for the inner solution, we posed the boundary conditions simply as a specified pressure directly at the surface. More precisely, the boundary conditions should represent an extrapolation of the continuum solution across the $\Delta\xi \sim Kn^2$ region adjacent to the wall (the 'Burnett sublayer') within which the Burnett equation is no longer valid. Makashev[22] and Schamberg[24] have derived boundary conditions that are consistent with the order–Kn^2 level of the Burnett equations. However, the accuracy of these approaches has not been rigorously established[18], nor are we aware of order–Kn^2 relations specifically for the pressure 'slip' at a heated or cooled surface. It should be noted that in application of the Burnett equations to 1–D hypersonic flow – which resulted in an improved description of shock structure relative to the Navier–Stokes solution – surface boundary conditions were obtained from order–Kn slip relations. The rationale for this approach was that the flow adjacent to the surfaces (within the Prandtl

boundary layer) could be well described in the Navier–Stokes level, and Burnett effects would only become significant within the shock wave itself.[10]

This is not the case in the problem examined here. as thermal stress will affect the pressure field throughout the heat flow domain. However, following the rationale used to develop the inner solution, we submit that an order–Kn pressure slip relation can be used as a boundary condition, providing that it is corrected for the order–Kn^2 bulk thermal stress effect in the Knudsen layer. Specifically, the quantity f_{1C} appearing in Eq. (21) would be related to the pressure slip at the cold surface via

$$f_{1C} = \left[\frac{1}{Kn}\left(\phi_C - \phi_{C,\infty}\right)\right]_{Kn\to 0} = -\phi_{C,\infty}\, c_p\, \theta'_C \tag{24}$$

in which $\phi_{C,\infty}$ is the 'freestream' pressure adjacent to the cold gas, θ'_C is the temperature gradient at the surface, and c_p is a constant. We now assume that $\phi_{C,\infty}$ is given by the bulk distribution averaged across the Knudsen layer, per the procedure in Eqs. (19) and (21). This results in

$$\phi_C = \tau^* \left(1 - Kn\, c_p\, \theta'_C\right) + Kn^2 \left(\frac{c_1 c_2 q^{*2}}{\bar{\theta}_C}\right) \tag{25}$$

The value of c_p can be estimated from the results of Loyalka[19] and Sone et al.[12], who calculated the distributions of temperature and density in the Knudsen layer of a heated, hard–sphere gas by numerical solution of the linearized Boltzmann equation. The pressure at the surface would be obtained from the product of temperature and density at the surface, which, to order Kn, yields $c_p = 0.1913$.

III. NUMERICAL COMPUTATION

A. Direct Simulation Monte Carlo method

The 1–D DSMC procedure used to calculate the density, temperature, and pressure is based on a code used in an earlier investigation[15], and follows that developed by Bird.[25] Because of the highly nonisothermal conditions of the simulations. a nonuniform grid was employed in which the length Δx of each cell (or control volume) was set at 0.025–0.1 of the local mean free path as estimated from the continuum temperature profile. This is equivalent to maintaining a nominally constant number of computational molecules per cell. Typically, 20 molecules were assigned per cell, and the time step in the simulations, Δt, was 0.0125–0.05 of the average collision time. Collisions between pairs of molecules in a cell were simulated using the no–time–counter approach.

Calculations proceeded from an initial equilibrium state corresponding to the reference temperature and pressure of the gas. Sampling of molecular properties was begun after a fixed period (typically around 1000 collision times) from the starting point, to eliminate bias in the final results from the initial state. Properties of the bulk gas (density, temperature, pressure) were obtained from time averages of molecular properties sampled from each cell. The heat flux and normal stress were obtained from recording of the net molecular momentum and kinetic energy transport at the boundaries.

All DSMC calculations were performed on a SUN Ultrasparc-I workstation. Presented results correspond to averages taken over $2 \times 10^7 - 4 \times 10^7$ times steps – which required run times of 3–5 days on our machine. The large amount of averaging was required to reduce the noise (i.e., natural fluctuations) in the pressure profiles to a point that allowed comparison with the theoretical, continuum–based predictions.

B. Numerical Solution of Continuum Model

A finite difference method was used to numerically solve Eqs. (13) and (25) (and the corresponding boundary condition at the heated surface) for the pressure distribution. The domain was discretized onto a uniform mesh, and central differences were used to represent the pressure derivatives. The resulting difference equations were solved iteratively for the nodal values of ϕ, using an initial value of τ^* estimated from Eq. (17). The integral of ϕ over the domain was then computed using a trapezoid rule, and this value was divided into τ^* to obtain a new estimate of the normal stress. The procedure was then repeated until the relative change in τ^* decreased below 10^{-6}. Note that the convergence in τ^* to a constant implies that the calculated pressure field obeys Eq. (15). The solution procedure was stable for all values of Kn and q^* presented here, and the calculated values of ϕ and τ^* were independent of the initial values used in the iterations. Typically, 200 mesh points were used in the calculations. In all cases, presented results are within 0.5% of the values obtained when the number of mesh points was doubled.

IV. RESULTS

We begin by examining the behavior of the gas that is contained between two solid, perfectly–accommodating surfaces. Dimensionless wall temperatures, for the DSMC calculations, were calculated from Eqs. (8) and (10) for set values of q^* and Kn. Three values of q^* (= 1.0, 1.5, and 2.0) and three of Kn (= 0.05, 0.10, and 0.20) were used in the simulations. Listed in Table I are the values of θ_{CS}, θ_C, θ_H, and θ_{HS}, calculated from the

slip/continuum relations, corresponding to the q^* and Kn combinations.

The simulations presented here can represent highly nonequilibrium conditions. In the case of $q^* = 1.5$ and $Kn = 0.2$, the ratio θ_{HS}/θ_{CS} – which represents the ratio of the hot and cold surface temperatures – is around 23. Although such temperature gradients are obviously not representative of 'common' heat transfer applications, we found it necessary to include these cases to create situations in which the effects of thermal stress on pressure became clearly apparent.

Figure 2 presents temperatures, calculated from DSMC simulations, for $q^* = 1.5$ and $Kn = 0.05$, 0.1 and 0.2. Shown also is the continuum prediction from Eq. (7). The dimensionless continuum prediction is independent of Kn – since it is based on the heat flux in the gas and not on the surface temperatures. The results are entirely consistent with previous DSMC investigations of 1–D heat transfer.[17,18] The DSMC and continuum temperatures are in good agreement in the bulk gas – which supports the accuracy of the temperature slip conditions. The breakdown of the continuum model is also clearly evident within the Knudsen layer adjacent to the hot wall – which, as expected, increases approximately linearly in thickness with increasing Kn.

Comparison of the DSMC and Burnett predictions of pressure distribution appear in Figs. 3–5. The quantity $\phi/\tau^* = P/\tau$, where τ is the DSMC–calculated normal stress, is plotted vs. ξ for $q^* = 1.0$ (Fig. 3), 1.5 (Fig. 4), and 2.0 (Fig. 5). The Knudsen number Kn is a parameter in each plot. We present ϕ/τ^*, rather than ϕ, in order to separate the curves and to illustrate the disparity between the pressure and the normal stress. Two theoretical predictions of P/τ are shown for each set of DSMC results. The first corresponds to the numerical solution of Eq. (13) with boundary conditions given by Eq. (25) and temperatures predicted from Eq. (7). The second represents the outer approximation given by Eq. (14), in which τ^* is predicted by Eq. (17). This second curve has been adjusted by a constant to match the numerical solution results at $\xi = 0.5$.

As is evident from the DSMC results, the pressure profiles show distinct Knudsen layers at both the cooled and heated surfaces, with pressure decreased and increased relative to the freestream values at the cold and hot surfaces, respectively. The pressure drop at the cold surface can be considerable for the conditions examined here – amounting to around an 8% decrease for $Kn = 0.2$ and $q^* = 1.5$.

The numerical solution of the Burnett equation, with the corrected slip boundary conditions, is seen to capture the essential features of the DSMC pressure distribution. In particular, the solution provides a reasonable description of the width and form of the

Knudsen layers and the pressure distribution outside the layers. The difference between the theoretical and DSMC results is greatest at the edge of the cold-surface Knudsen layers, and, as expected, this difference increases with increasing Kn and q^*. The same trends are seen in the differences between the DSMC pressures at the surface and those calculated by Eq. (25), yet this difference is no larger than 10%, on a relative basis, for the conditions examined here. We also examined solutions to Eq. (13) in which the thermal stress correction was removed from Eq. (25), and these results were in considerably less agreement with the DSMC values. Furthermore, solutions to Eq. (13) that used boundary conditions derived from the DSMC pressures at the surface (i.e., 'exact' boundary conditions) did not result in a significantly better fit with the DSMC pressure distributions than those generated with Eq. (25).

A comparison of the DSMC, numerical Burnett solution, and composite inner asymptotic approximation of Eq. (23) is presented in Fig. 6, for the conditions given in Fig. 4 (i.e., $q^* = 1.5$). We use a value of τ^* in Eq. (23) corresponding to that predicted from Eq. (17) and boundary conditions at $\xi = 0$ are obtained from Eq. (25). Note that Eq. (15) would not hold for Eq. (23), since the solution cannot match both boundary conditions. Results are shown for $\xi = 0$ to 0.2. The inner and full-Burnett solutions are practically indistinguishable for $Kn = 0.05$ and 0.1, yet for $Kn = 0.2$ there is a substantial divergence between the two results in the freestream. This latter difference indicates that 'bulk' conditions are not attained for the given conditions, i.e., the Knudsen layers affect the pressure distribution throughout the heat flow domain. The same conclusion can be inferred from comparison of the outer approximations and Burnett predictions in Figs. 3 and 4 for $Kn = 0.2$. On the other hand, the outer distribution in pressure is evident in the results for smaller Kn (i.e., Fig. 5).

As can be theoretically inferred from Eq. (23), as well as by inspection of Figs. 3 and 5, decreasing Kn while maintaining $Kn\, q^*$ constant results in progressively narrower Knudsen layers, for which the effects of thermal stress in the bulk gas can be better observed. It would be impractical to perform DSMC calculation for values of q^* much larger than the maximum of 2.0 used here. We can, however, alter the DSMC boundary conditions at $\xi = 1$ to model molecular conditions in the bulk gas, as opposed to molecular reflection from a solid surface. This approach will, in principle, eliminate the Knudsen layer effects at $\xi = 1$, and thus better isolate the effects of thermal stress.

Following this rationale, we performed additional DSMC calculations on the 'open' boundary system. To maintain zero net mass flux at the $\xi = 1$ boundary, a new molecule

was released into the system every time a molecule left the system by crossing $\xi = 1$. The velocity components of the released molecule were randomly sampled from a Chapman-Enskog distribution function, with probability given by

$$p(u^*, s^*) = -u^* s^* e^{-u^{*2}-s^{*2}} \left[1 - Du^* \left(u^{*2} + s^{*2} - \frac{5}{2}\right)\right] \tag{26}$$

In the above,

$$u^* = \frac{u}{\sqrt{2RT_H}} \tag{27}$$

is the dimensionless axial thermal velocity of the molecule, $s^* = \sqrt{v^{*2} + w^{*2}}$ is the dimensionless radial molecular velocity, and

$$D = \frac{15\sqrt{\pi}}{16} \frac{\lambda}{T_H} \left.\frac{dT}{dx}\right|_{x=L} = \frac{15\sqrt{\pi}}{16} \frac{Knq^*}{\theta_H^{1/2}} \tag{28}$$

Note that the constant D is chosen to simulate a heat flux of q^* entering through the hot boundary, which is maintained at a temperature of θ_H. An acceptance–rejection procedure was used to sample velocities from Eq. (26). Aside from the changed distribution function, the computational procedure remained the same as before. Calculations were performed for $Kn = 0.1$ (i.e., the system outer boundary is located at $10\lambda_{ref}$), and q^* was set to 1.0, 1.5, and 2.0. The value of θ_H used in Eq. (26) is the same as that listed in Table I for the corresponding value of q^*. For $q^* = 2.0$, the value of D is 0.228 – which is near the limit of validity of the Chapman–Enskog distribution function.[25]

DSMC results of temperature for the open-boundary system, and the continuum predictions given by Eq. (7), appear in Fig. 7. Knudsen layers are no longer observed at $\xi = 1$, which is indicated by the close correspondence of the DSMC and continuum predictions throughout the system. Pressure distribution results are plotted in Fig. 8. Theoretical predictions again correspond to the full solution of Eq. (13) and the outer approximation of Eq. (14). The boundary condition at $\xi = 1$ for the numerical solution has now been changed to remove the slip effect (i.e., $c_p = 0$ in Eq. (25) for $\xi = 1$). As was the case with the temperature profiles, the DSMC pressure distributions do not show the presence of Knudsen layer effects at $\xi = 1$. For $q^* \leq 1.5$, the DSMC pressure distribution in the bulk gas is seen to correspond closely to the prediction of Eq. (14) – which in turn matches the distribution predicted by the full solution of Eq. (13). These results indicate that the bulk–gas pressure distribution is a direct effect of temperature gradients within the gas – and is not the result of nonequilibrium at the surfaces.

A final comparison of theory and experiment can be obtained from the dimensionless normal stress. The simplified model of Eq. (17) indicates that τ^* should be a function primarily of $Kn\,q^*$. Accordingly, we plot in Fig. 9 the DSMC values of τ^* vs. $Kn\,q^*$ for the seven different combinations of Kn and q^* that were used in the closed system calculations (results of Figs. 3–5). Theoretical results correspond to the derived eigenvalues of Eq. (13) and to the approximation given by Eq. (17).

The first point to make is that the predictions of τ^* from full solution of the Burnett differential equation are closely equivalent to those obtained from the outer approximation of Eq. (17). Evidently, the decrease in pressure at the cold surface is compensated by the increase at the hot, so that the Knudsen layers have a small effect on the averaged pressure in the gas. Secondly, the primary dependence of τ^* on $Kn\,q^*$ is supported in the DSMC results at $Kn\,q^* = 0.1$ and 0.2 – which each correspond to two combinations of Kn and q^*. As observed, the results are nearly identical at these points. Finally, the theoretical predictions are in excellent agreement with the DSMC results for $Kn\,q^* \leq 0.15$, beyond which the theory overpredicts the decrease in τ^*. As can be seen from the results, the relative decrease in normal stress on the surfaces is quite small, i.e., $\tau^* = 0.975$ for $q^* = 2.0$ and $Kn = 0.2$, or a 2.5% decrease in 'measured' pressure at the surface. We should emphasize, however, that this decrease is still significantly larger than the numerical precision of the DSMC simulations.

V. SUMMARY

This investigation has compared Burnett equation predictions of pressure distribution and normal stress with DSMC results for 1–D heat transfer in a stationary, hard–sphere gas. For $Kn\,q^*$ less than around $0.1 - 0.15$, our results show that the theoretical pressure profiles can reasonably match those obtained from DSMC. The pressure distribution within the Knudsen layer is consistent with an order–Kn asymptotic solution of the Burnett equation. Likewise, a simplified outer solution to the Burnett equation, which neglects Knudsen layer effects at the surfaces, gives an accurate prediction of the reduction in normal stress due to thermal stress, for the same constraint on $Kn\,q^*$.

We conclude by emphasizing that our findings do not imply that the Burnett equations and the derived pressure boundary conditions will remain valid when applied to more complicated heat and momentum transfer configurations - such as those involving gas flows and velocity gradients. Indeed, the stationary, 1–D system examined here probably represents the most simple configuration in which thermal stress effects could be isolated.

In this sense, a fatal flaw in the Burnett equations would have been revealed by a lack of correspondence between the experimental (i.e., DSMC) observations and theoretical predictions of pressure and stress in this system. The results of this investigation, however, prove otherwise, and hopefully will encourage others to examine the veracity and usefulness of the Burnett equations in practical rarefied gas dynamics applications.

Acknowledgements

This work was supported by the National Aeronautics and Space Administration, Microgravity Fluid Physics Program, Contracts NAG3–1882 (DWM) and NAG3–1951 (DHP and DER), R. Balasubramanian, technical officer.

[1] D. Burnett, "The distribution of molecular velocities and the mean motion in a non–uniform gas," *Proc. Lond. Math. Soc* **40**, 382 (1935).

[2] S. Chapman, and T. G. Cowling, *The Mathematical Theory of Non–Uniform Gases* (Cambridge University Press, London, 1970).

[3] C. Cergignani, *Mathematical Methods in Kinetic Theory*, Second Edition (Plenum Press, New York, 1990), ch. 5.

[4] C. J. Lee, "Unique determination of solutions to the Burnett equations," *AIAA J.* **32**, 985 (1994).

[5] L. A. Woods, *An Introduction to the Kinetic Theory of Gases and Magnetoplasmas*, Oxford University Press, 1993.

[6] K. A. Comeaux, R. W. MacCormack, and D. R. Chapman. "An Analysis of the Burnett Equations Based on the Second Law of Thermodynamics," AIAA 33rd Aerospace Sciences Meeting and Exhibit, 9–12 January 1995, Reno, NV, paper 95–0415.

[7] K. A. Fisko and D. R. Chapman, "Comparison of Burnett, Super–Burnett, and Monte–Carlo solutions for hypersonic shock structure," *Rarefied Gas Dynamics: Theoretical and Computational Techniques*, E. P. Muntz, D. P. Weaver, and D. H. Campbell, Eds., Vol. 118, Progress in Astronautics and Aeronautics, 1989, pp. 374–395.

[8] G. C. Pham–Van–Diep, D. A. Erwin, and E. P. Muntz, "Testing continuum descriptions of low–Mach–number shock structures," *J. Fluid Mech.* **232**, 403 (1991).

[9] F. E. Lumpkin and D. R. Chapman, "Accuracy of the Burnett equations for hypersonic

real gas flows," *J. Thermophysics Heat Transfer* **6**, 419 (1992).

[10] X. Zhong, R. W. MacCormack, and D. R. Chapman, "Stabilization of the Burnett equations and application to hypersonic flows," *AIAA J.* **31**, 1036 (1993).

[11] M. N. Kogan, "Molecular Gas Dynamics," in *Annual Review of Fluid Mechanics*, M. Van Dyke and W. G. Vincenti, Eds., Annual Review, Palo Alto, 1973, Vol. 5, pp. 383.

[12] Y. Sone, "Flow induced by thermal stress in rarefied gas," *Phys. Fluids* **15**, 1418 (1972).

[13] D. E. Rosner, "Side wall gas 'creep' and 'thermal stress convection in microgravity experiments on film growth by vapor transport," *Phys. Fluids* **A1**, 1761 (1989).

[14] A. Viviani and R. Savino, "Recent developments in vapour crystal growth fluid dynamics," *J. Crystal Growth* **133**, 217 (1993).

[15] D. H. Papadopoulos and D. E. Rosner, "Enclosure gas flows driven by non–isothermal walls," *Phys. Fluids* **7**, 2535 (1995).

[16] D. W. Mackowski, V. R. Rao, D. G. Walker, and R. W. Knight, "Numerical investigation of the effects of thermal creep in physical vapor transport," *J. Crystal Growth* **179**, 297 (1997).

[17] D. C. Wadsworth, "Slip effects in a confined rarefied gas. I: temperature slip," *Phys. Fluids A* **5**, 1831 (1993).

[18] X. Zhong and K. Koura, "Comparison of solutions of the Burnett equations, Navier–Stokes equations, and DSMC for Couette flow," *Twentieth International Symposium on Rarefied Gas Dynamics*, Bejing, 1996.

[19] S. K. Loyalka, "Temperature jump and thermal creep slip: rigid sphere gas," *Phys. Fluids A* **1**, 403 (1989).

[20] D. E. Rosner and D. H. Papadopoulos, "Jump, slip, and creep boundary conditions at nonequilibrium gas/solid interfaces," *I&EC Res.* **35**, 3210 (1996).

[21] M. N. Kogan, *Rarefied Gas Dynamics* (Plenum Press, New York, 1969), ch. 3.

[22] N. K. Makashev, "On the boundary conditions for the equations of gas dynamics corresponding to the higher approximations in the Chapman–Enskog method of solution of the Boltzmann equation," *Fluid Dyn.* **14**, 385 (1979).

[23] J. C. Maxwell, "On the stresses in rarefied gases arising from inequalities of temper-

ature (appendix)," *Philos. Trans. Roy. Soc. Lond.* **170**, 231 (1979).

[24] R. Schamberg, "The fundamental difference equations and the boundary conditions for high speed slip flow," Ph.D. Thesis, California Inst. Tech., Pasadena, CA, 1947.

[25] G. A. Bird, *Molecular Gas Dynamics and the Direct Simulation of Gas Flows* , (Oxford, Clarendon Press, 1994).

q^*	Kn	θ_{CS}	θ_C	θ_H	θ_{HS}
1.0	0.10	0.4451	0.5469	1.5364	1.7791
1.0	0.20	0.3753	0.5469	1.5364	2.1129
1.5	0.05	0.2986	0.3615	1.8260	2.0151
1.5	0.10	0.2543	0.3615	1.8260	2.2479
1.5	0.20	0.1961	0.3615	1.8260	2.9235
2.0	0.05	0.1528	0.2092	2.1241	2.4029
2.0	0.10	0.1203	0.2092	2.1241	2.7659

TABLE I. Dimensionless surface and gas temperatures.

Figure Captions

1. Problem schematic
2. DSMC and continuum dimensionless temperature distributions vs. dimensionless position, $q^* = 1.0$.
3. DSMC and continuum pressure distributions, vs. dimensionless position, $q^* = 1.0$.
4. DSMC and continuum pressure distributions, vs. dimensionless position, $q^* = 1.5$.
5. DSMC and continuum pressure distributions, vs. dimensionless position, $q^* = 2.0$.
6. DSMC, exact Burnett, and asymptotic approximation pressure distributions, vs. dimensionless position, $q^* = 1.5$.
7. DSMC and continuum temperature distributions, open system.
8. DSMC and continuum pressure distributions, open system.
9. DSMC and continuum predictions of dimensionless normal stress, vs. $Kn\, q^*$.

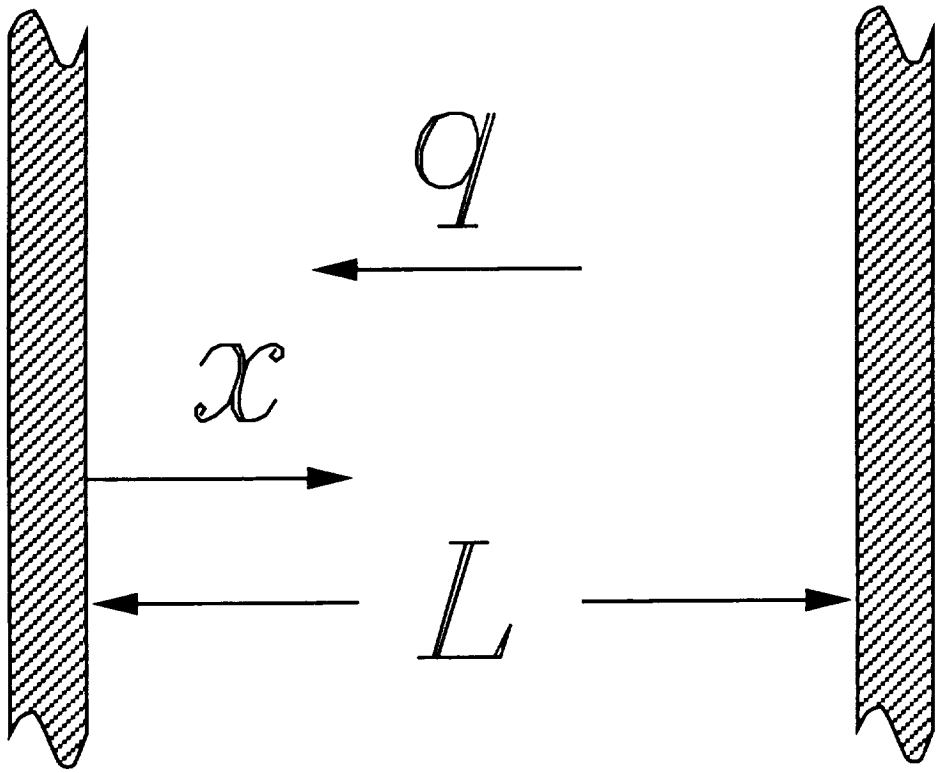

Fig. 1

Mackowski et al.

PF 5007A

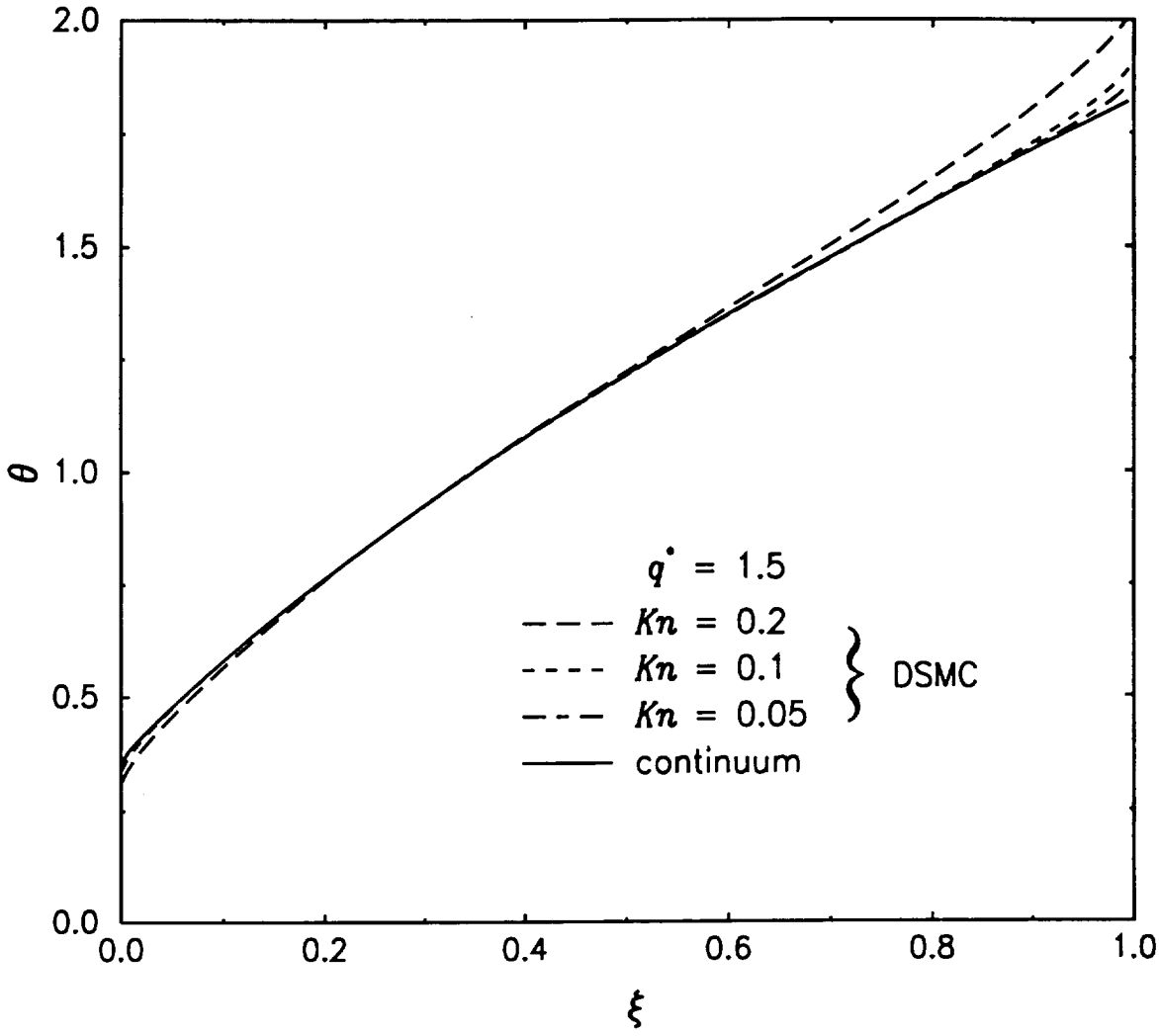

Fig. 2

Mackowski et al.

PF 5007A

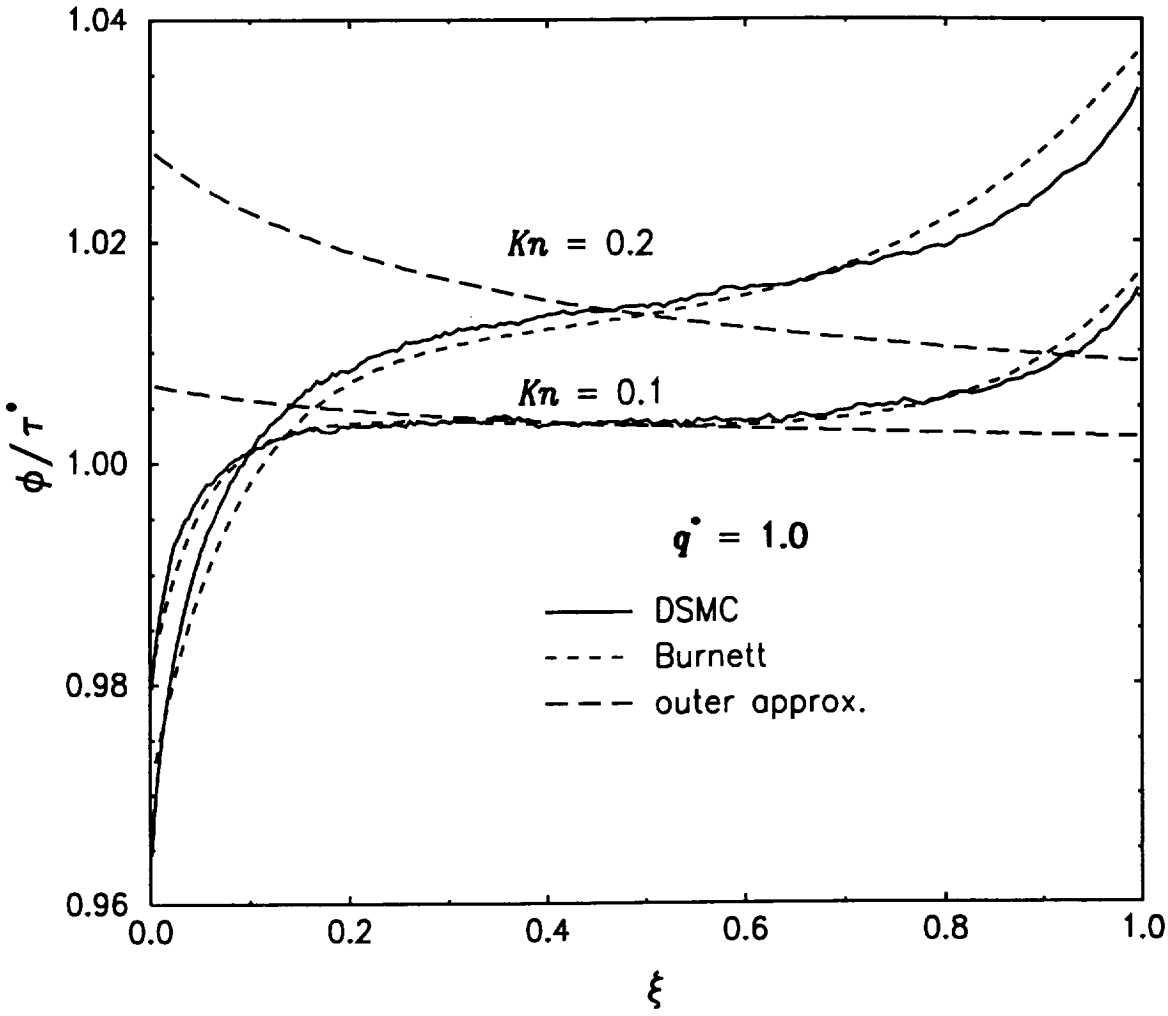

Fig. 3

Mackowski et al.

PF 5007A

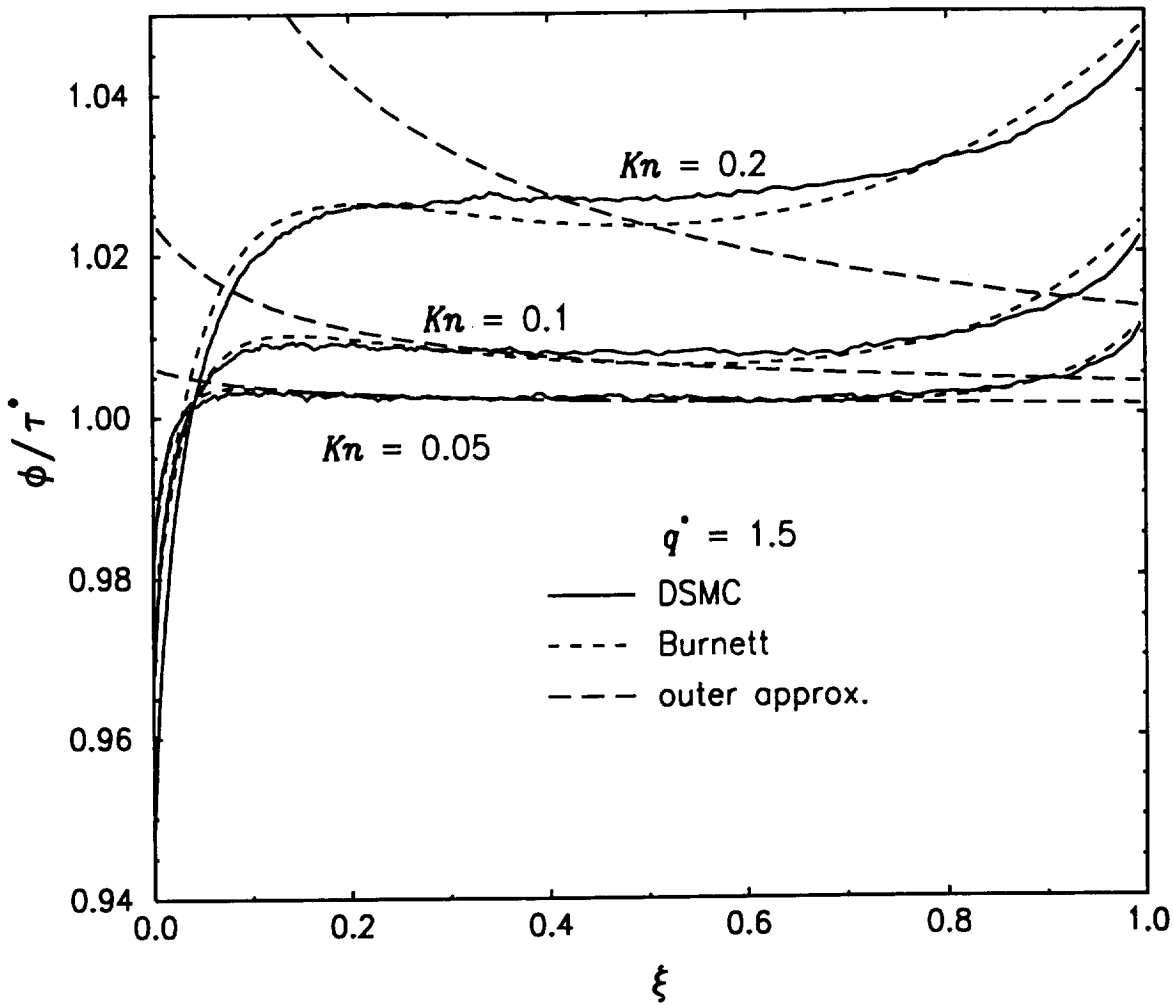

Fig. 4

Mackowski et al.

PF 5007A

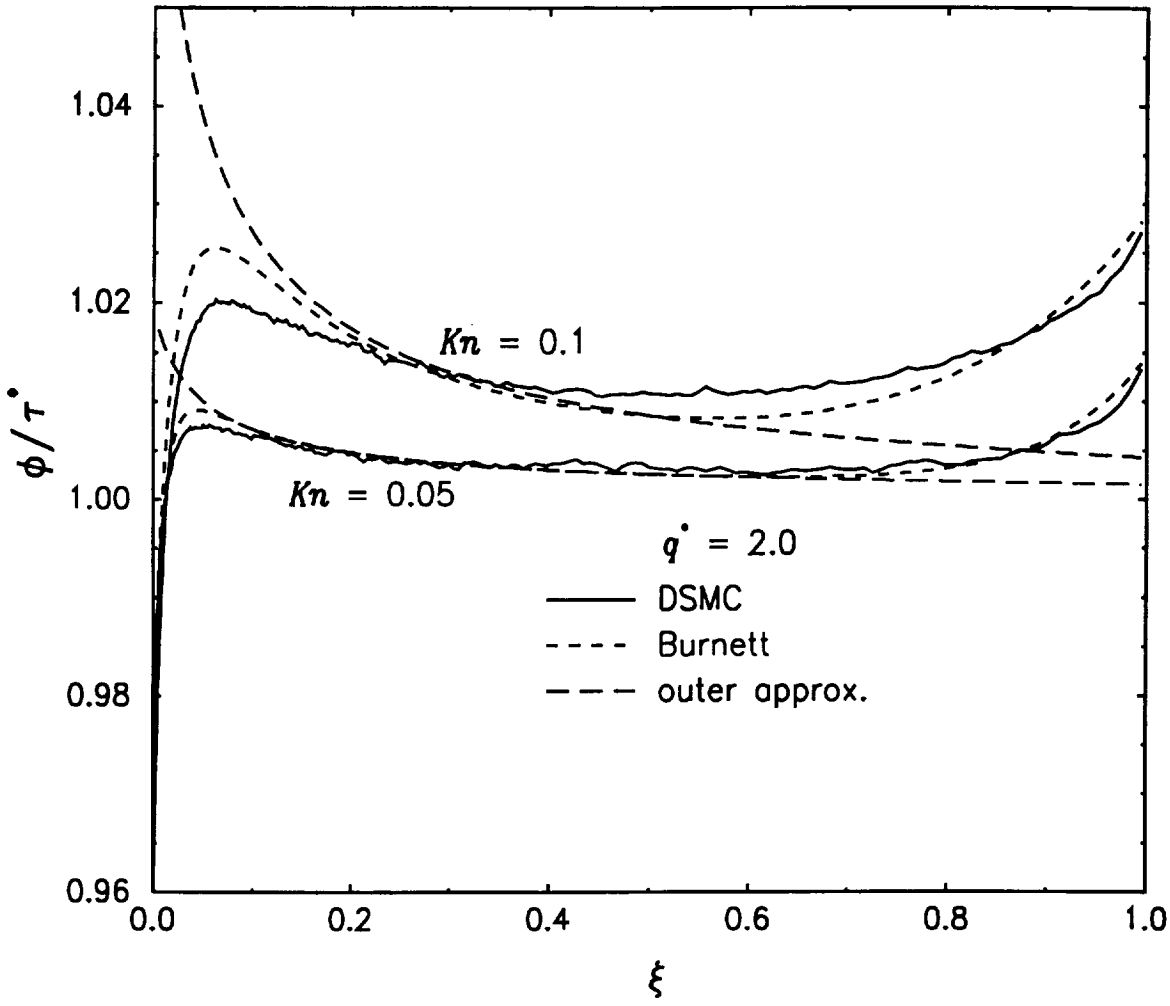

Fig. 5

Mackowski et al.

PF 5007A

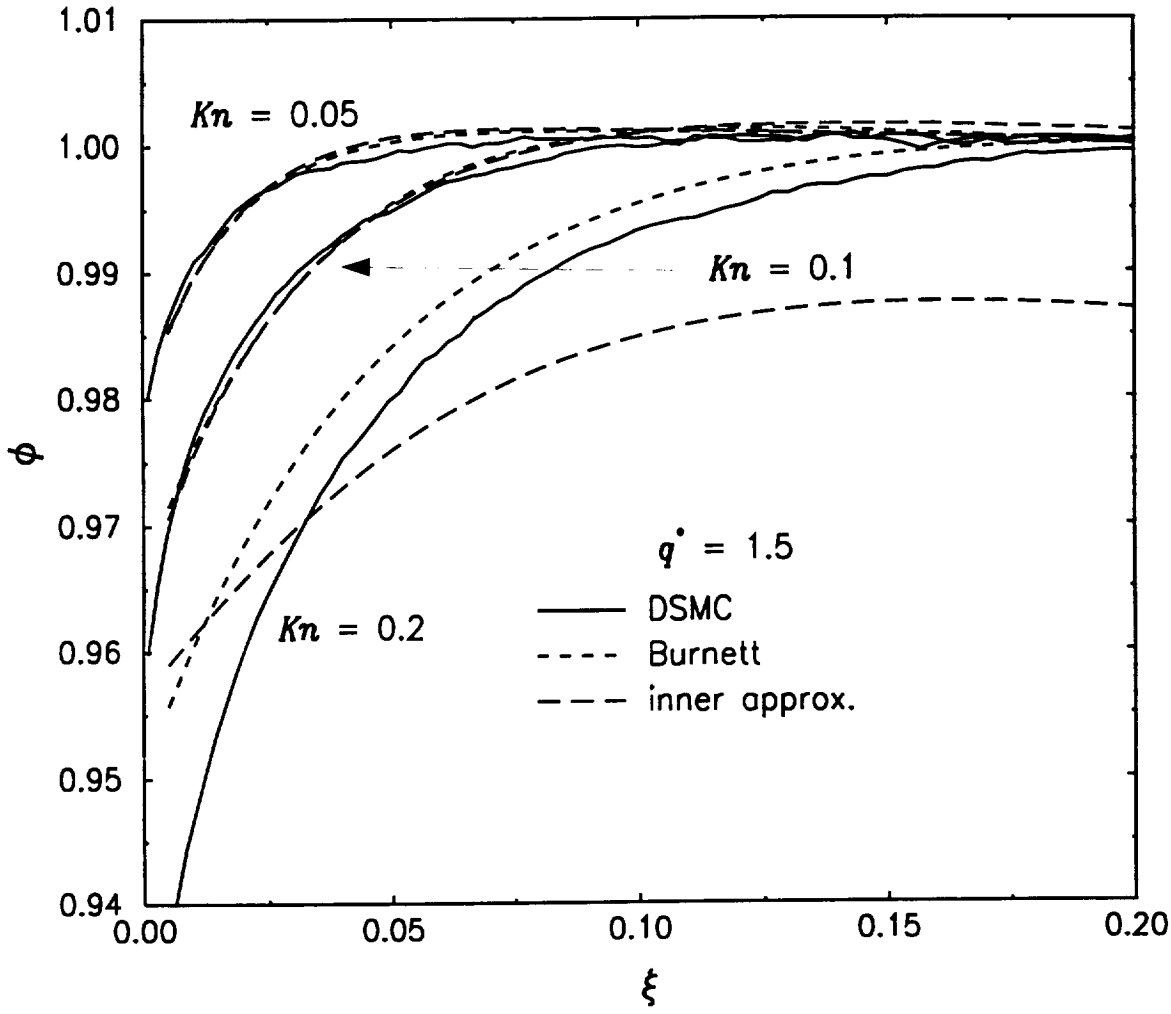

Fig. 6

Mackowski et al.

PF 5007A

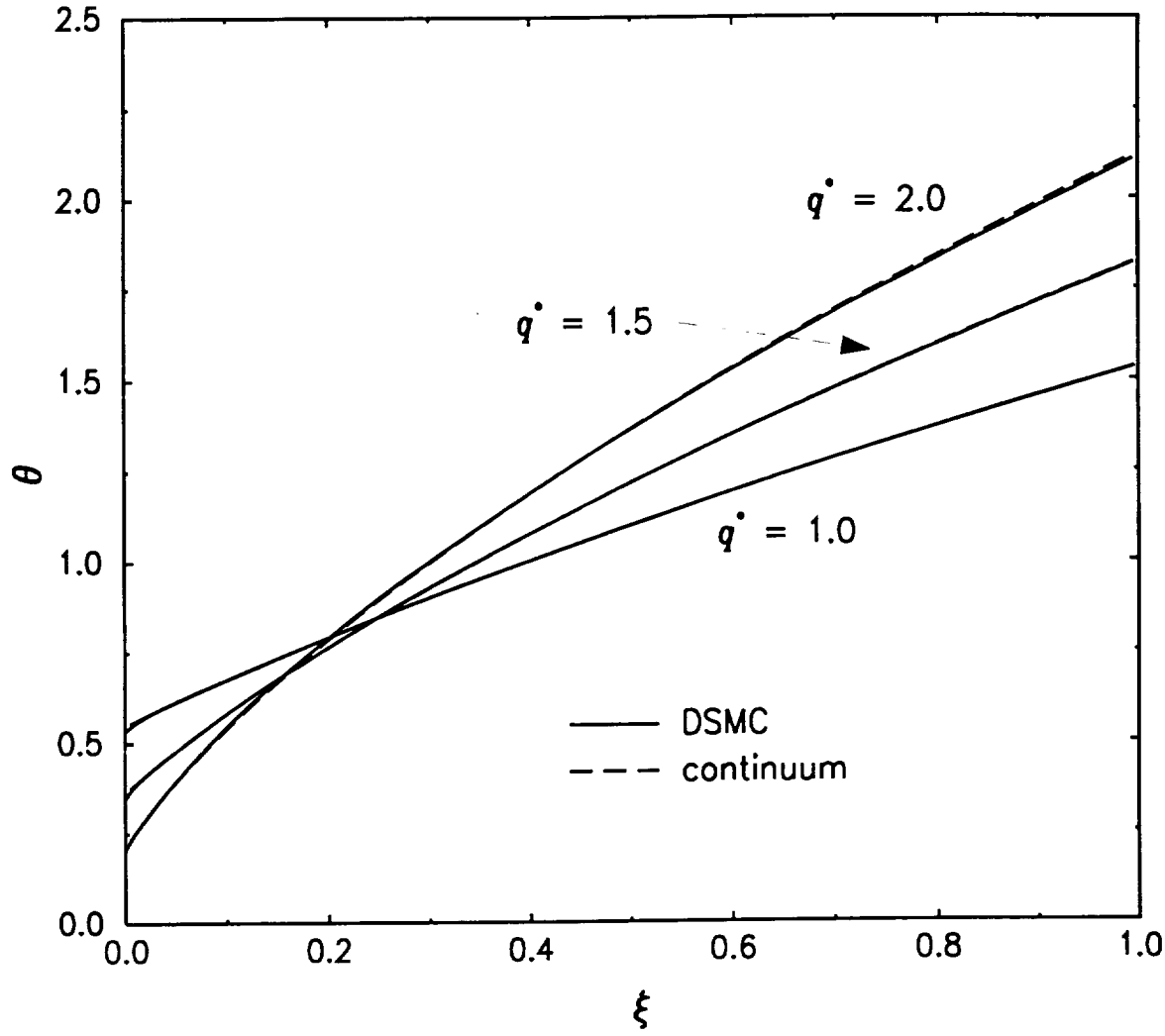

Fig. 7

Mackowski et al.

PF 5007A

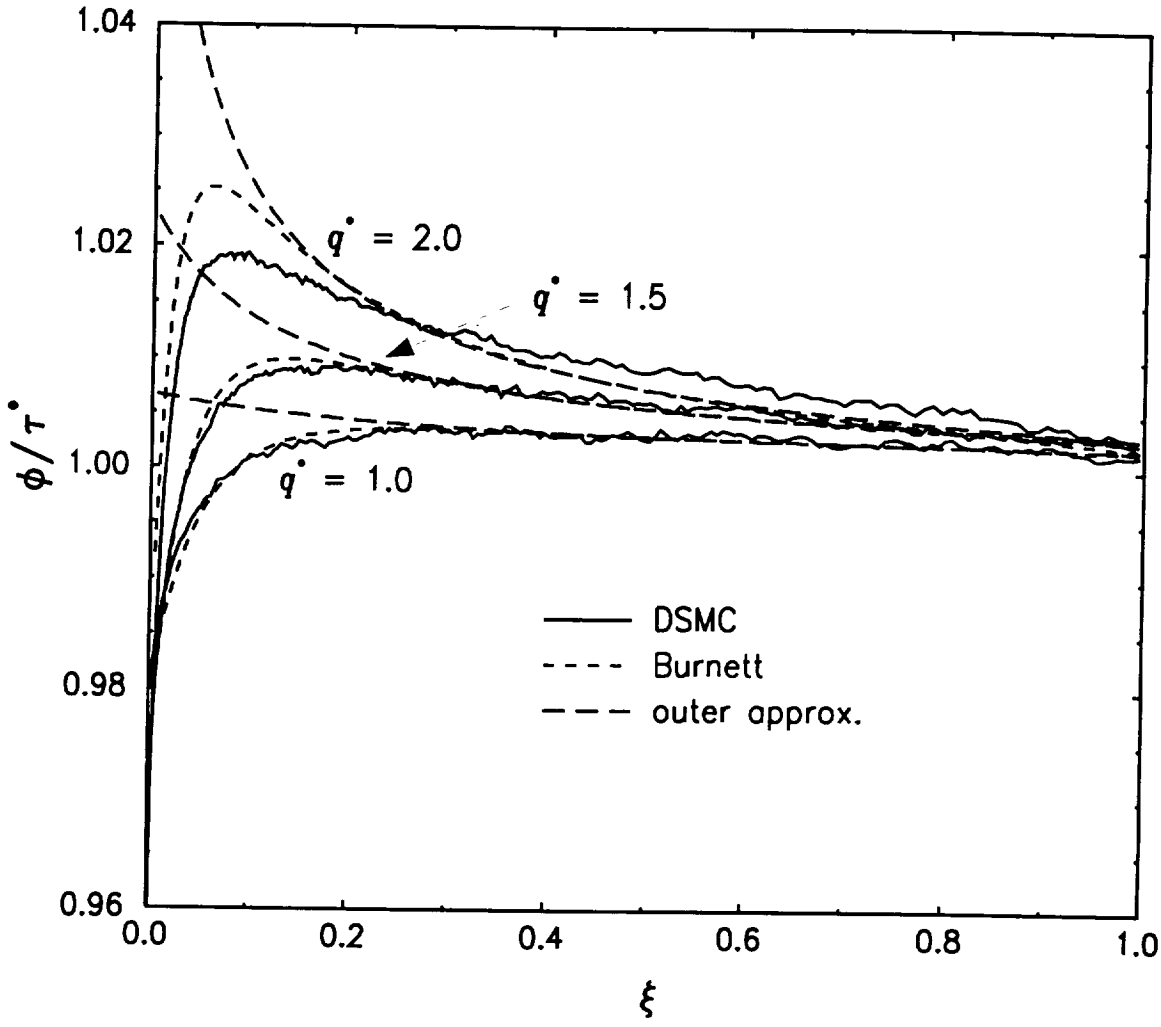

Fig. 8

Mackowski et al.

PF 5007A

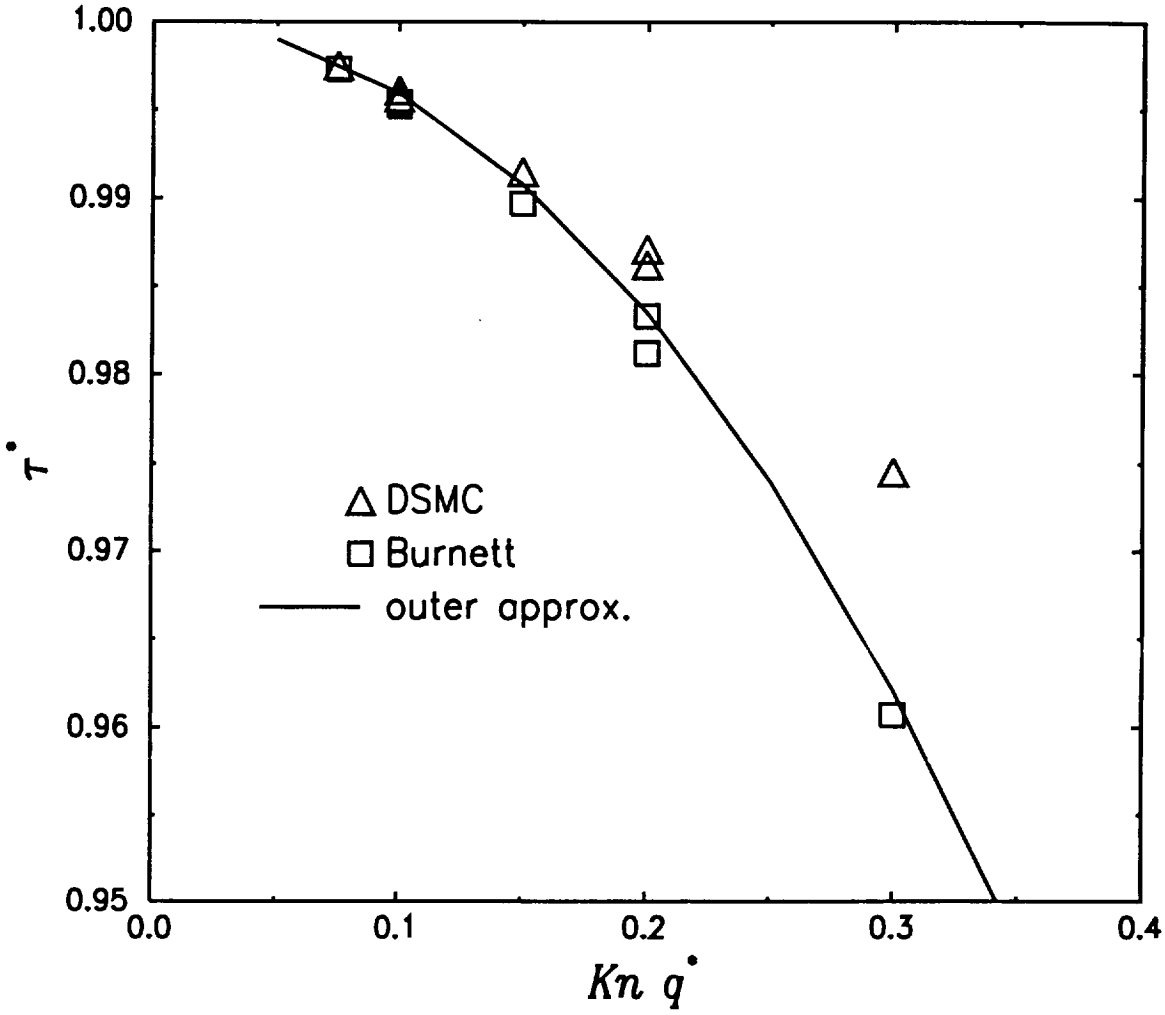

Fig. 9

Mackowski et al.

PF 5007A